A high level of TGF-B1 promotes endometriosis development via cell migration, adhesiveness, colonization, and invasiveness.

Running title: TGF-B1 is involved in endometriosis development.

Summary sentence: TGF-B1 regulates the pathophysiology of endometriosis by specifically enhancing the migration, attachment, proliferation, colonization, and invasiveness of floating endometriotic cells or tissues, via the integrin-FAK, cadherin, and RHOGTPase signaling cascades.

Keywords: Peritoneal-endometriosis, TGF-B1, Integrins, Cadherins, Focal Adhesion Kinase (FAK), RHOGTPase, EMT, cell migration, colonization, 3D-spheroids, invasion.

Abbreviation: TGF-B1-(Transforming Growth Factor-B1), Eu-(eutopic), Ec-(ectopic), EMT-(Epithelial-Mesenchymal Transition), ITGB-(Integrin beta), FAK-(Focal Adhesion Kinase), FMT-(Fibroblast-Myo-fibroblast transition), HRP-(Horseradish peroxidase).

Funding: This research work was supported in part by NWP, BSC0103, CSIR and Department of Biotechnology, (DBT, BT/PR14480/ MED/ 97/ 265/2015), New Delhi, India. Upendra Kumar Soni is awarded with the fellowship from Council of Scientific and Industrial Research (CSIR), New Delhi, India (21/12/2014(ii) EU-v). Research fellowships awarded to Chadchan Sangappa Basanna was from Indian Council of Medical Research (ICMR), New Delhi, India (3/1/3/JRF-2011/ HRD-75, 61102) and Vijay Kumar and Vaibhave Ubba fellowships were from and University Grant Commission (UGC), New Delhi, India respectively.

Authors: Upendra Kumar Soni[1#], Sangappa Basanna Chadchan[1#], Vijay Kumar[1], Vaibhave Ubba[1], Mohammad Tariq Ali Khan[1], Budai Shanmukha Vivek Vinod[1], Rituraj Konwar[1], Himangsu Kousik Bora[2], Srikanth Kumar Rath[3], Sharad Sharma[3], Rajesh Kumar Jha[1*].

Authors Affiliations

[1] Endocrinology Division, CSIR-Central Drug Research Institute, Lucknow-226031, India.

[2] Animal Laboratory Division, CSIR-Central Drug Research Institute, Lucknow-226031, India.

[3]Toxicology and Experimental Medicine Division, CSIR-Central Drug Research Institute, Lucknow-226031, India.

# Upendra Kumar Soni and Sangappa Basanna Chadchan contributed equally to this work.

[*]**Corresponding Author**

Rajesh Kumar Jha, Ph.D.

Senior Scientist,

Downloaded from https://academic.oup.com/biolreprod/advance-article-abstract/doi/10.1093/biolre/ioy242/5181331 by EKU Libraries user on 14 November 2018

Endocrinology Division,

Life Science North 111B/101,

CSIR-Central Drug Research Institute

B.S. 10/1, Sector-10, Jankipuram Extension,

Sitapur Road, Lucknow-226031, India

Tele: +91-7376818092 , 0522-2772450, 2772550 Ext. 4493

Email ID: rajesh_jha@cdri.res.in

Web page: http://www.cdri.res.in/1769.aspx?id=1769

https://scholar.google.co.in/citations?user=WWMaowwAAAAJ&hl=en

Abstract

Endometriosis is a prevalent gynecological disorder that eventually gives rise to painful invasive lesions. Increased levels of transforming growth factor-beta1 (TGF-B1) have been reported in endometriosis. However, details of the effects of high TGF-B1 on downstream signaling in ectopic endometrial tissue remain obscure. We induced endometriotic lesions in mice by surgical auto-transplantation of endometrial tissues to the peritoneal regions. We then treated endometriotic (ectopic and eutopic endometrial tissues) and non-endometriotic (only eutopic endometrial tissues) animal groups with either active TGF-B1 or PBS. Our results demonstrate that externally supplemented TGF-B1 increases the growth of ectopically implanted endometrial tissues in mice, possibly via SMAD2/3 activation and PTEN suppression. Adhesion molecules integrins (beta3 and beta8) and FAK were upregulated in the ectopic endometrial tissue when TGF-B1 was administered. Phosphorylated E-cadherin, N-cadherin, and vimentin were enhanced in the ectopic endometrial tissue in the presence of TGF-B1 in the mouse model**,** and correlated with Epithelial-Mesenchymal Transition (EMT) in ovarian endometriotic cells of human origin. Further, in response to TGF-B1, the expression of RHOGTPases (RAC1, RHOC and RHOG) were increased in the human endometriotic cells

Downloaded from https://academic.oup.com/biolreprod/advance-article-abstract/doi/10.1093/biolre/ioy242/5181331 by EKU Libraries user on 14 November 2018

(ovarian cyst derived cells from endometriosis patient) and tissues from the mouse model of endometriosis (ectopic endometrial tissue). TGF-B1 enhanced the migration, invasive, and colonizing potential of human endometriotic cells. Therefore, we conclude that TGF-B1 potentiates the adhesion of ectopic endometrial cells/tissues in the peritoneal region by enhancing the integrin- and FAK-signaling axis, and also migration via cadherin-mediated EMT and RHOGTPase–signaling cascades.

1. Introduction

Endometriosis is an estrogen-dependent gynecological disorder in which floating endometrial tissue proliferates, migrates, attaches to, colonizes, and invades ectopic/extra-uterine sites (such as the pelvic peritoneum, mesentery area, ovarian cortex, and rectovaginal septum). This eventually leads to severe pelvic pain due to the formation of endometriotic lesions and chronic inflammation [1]. Female infertility is also associated with endometriosis. The prevalence of endometriosis ranges from 10-14% in women of reproductive age. However, the frequency of its occurrence increases to 35–50% among patients with pelvic pain and infertility [2]. Retrograde menstrual dissemination of endometrial tissue was initially hypothesized to be the cause of endometriosis histogenesis [3]; however, other factors such as an imbalance in steroid hormone-signaling in the endometrial tissue, impaired immune function, and epigenetic changes triggered by environmental toxicants, have subsequently been implicated [2].

The precise molecular pathways that allow the establishment and survival of the endometrial cells at ectopic sites remain poorly understood, leading endometriosis to be labeled an enigmatic disease. Estradiol participates in the development of endometriosis by promoting cell invasion through activation of the beta-catenin signaling pathway [4]. Estradiol is also a critical mediator of macrophage-nerve cross-talk in peritoneal endometriosis [5]. Endometrium-

Downloaded from https://academic.oup.com/biolreprod/advance-article-abstract/doi/10.1093/biolre/ioy242/5181331 by EKU Libraries user on 14 November 2018

derived cells form the ectopic cyst/tumor-like structures which give rise to the endometriotic lesions [6]. Epithelial-mesenchymal transition (EMT) of these ectopic cells is one of the important events required for the development of the endometriotic lesions. The resulting endometriotic cells are notoriously resistant to apoptosis and show accelerated proliferation [7].

The pleiotropic cytokine, transforming growth factor–beta (TGF-B1), is expressed in endometriosis, and its increased expression is critical to various pathways of endometriosis development [8]. TGF-B1 levels in the peritoneal fluid (PF) of endometriosis patients were elevated to a concentration of ~1550 pg/mL, while healthy individuals had a corresponding level of ~1100 pg/mL [9]. Unavailability of TGF-B1 completely abolishes the development of endometriotic lesions in the mouse model of endometriosis [10]. TGF-B1 also promotes EMT and FMT (Fibroblast-Myo-fibroblast transition) in endometriosis, and results in increased cell contractility, collagen production, and ultimately leads to fibrosis [11]. Recently, TGF-B1 was found to regulate angiogenesis and inflammation in the human endometriosis [9;12]; this in turn provides a favorable microenvironment to attach the floating uterine remnants at ectopic sites. Immune-escape of endometriotic cells facilitates cellular adhesion [13] and invasion of endometriotic cells at the peritoneal sites [14], and is considered an important mechanism for the development of endometriosis. It has been reported that macrophages become activated in endometriosis and regulate the genesis of endometriotic lesions [15]. Interestingly, TGF-B1, which is primarily secreted by activated macrophages [13;16] but also locally by endometrial cells [17], can regulate immune-escape of endometriotic cells as well [18]. In sum, studies in mice and women have indicated that increased levels of TGF-B1 are associated with decreased immune cell activity within the peritoneum, along with an increase in ectopic endometrial cell survival, attachment, invasion, and proliferation during endometriosis lesion development. TGF-

Downloaded from https://academic.oup.com/biolreprod/advance-article-abstract/doi/10.1093/biolre/ioy242/5181331 by EKU Libraries user on 14 November 2018

B1 has a well-established role in the suppression of immune surveillance in tumors, thereby promoting the process of cancer metastasis [19]. Given this evidence, it would be interesting to examine if immune-escape of endometriotic cells employs similar mechanisms.

TGF-B1 binds the type I/II receptor complex on the membrane and activates downstream effectors via either the SMAD2/3 dependent pathway (canonical) or the SMAD-independent i.e. TAK1-p38MAPK signaling (non-canonical) axis [20;21]. TGF-B1 can induce the expression of integrin [22], which may in turn participate in cellular responses such as cell adhesion, cell survival, proliferation, differentiation, and migration. In endometriosis, differential expression of integrins – alpha1, alpha3, alpha6, alpha-v, beta1, and beta3, have been reported [23]. Active integrins transduce the signals to focal adhesion kinase (FAK) by phosphorylating Tyrosine 397 of FAK [24]. There has been recent speculation about the role of FAK in the pathogenesis of endometriosis [25]. FAK activation can induce the RHO-family of GTPases to regulate cell migration and adhesion events via various signaling intermediates [26]. Several RHOGTPases such as RHOA, RAC1, RHOC, and RHOG also facilitate integrin-FAK signaling [27;28]. RHOGTPases are also known to function in response to TGF-B1 signaling in various other cell types [29]. However, it is not yet clear whether TGF-B1 can act upon these molecules in the pathological development of endometriosis.

Succinctly, a crosstalk between integrin-TGF-B1 signaling cascades possibly regulates various cellular functions and disease pathology; however, the importance of this particular crosstalk has not yet been explored in the context of endometriosis. Therefore, this study was undertaken to decipher the underlying molecular mechanism for the pathogenesis of endometriosis with an emphasis on elucidating the effect of elevated TGF-B1 on cell adhesion,

Downloaded from https://academic.oup.com/biolreprod/advance-article-abstract/doi/10.1093/biolre/ioy242/5181331 by EKU Libraries user on 14 November 2018

endometrial cell migration, colonization, and invasion, using *in vitro* and *in vivo* models of endometriosis.

2. Materials and Methods

2.1 Animal model based investigations

2.1.1 Murine model of endometriosis: The peritoneal endometriosis mouse model (*Mus musculus*, Swiss strains) was developed by auto-transplantation of uterine tissue as previously described [30-32]. The study was conducted in according to the Institutional Animal Ethical Committee guidelines at Council of Scientific and Industrial Research-Central Drug Research Institute (CSIR-CDRI), Lucknow (IAEC/2012/108/ Renew-3(98/15)/dated-23/07/ 2015). After confirming the stage of the estrous cycle, an approximately 1.0 cm segment of one uterine horn was removed from each mouse anesthetized with ketamine (30mg/kg) and xylazine (4.0mg/kg), and slit longitudinally. After removing the fat tissue and myometrium from uterine tissue [30;33], the endometrial tissue was cut into ~20-25mm^2 sizes in DMEM-F-12 supplemented with 1.0% antibiotics and antimycotics, and patched into the bilateral abdominal wall of the animal using surgical thread [31]. One week after surgery, one group of animals received 10 µl of an intra-peritoneal dose of active recombinant mTGF-B1 (5231, Cell Signaling Technology Inc., MA, USA) (14 ng/ml) [34] daily up to 14 days, while the other group (control sham-operated group) received PBS.

2.1.2 Macroscopic measurement of endometriotic lesions: All animals were euthanized by cervical dislocation on the 22nd day after endometriosis induction. The area of endometrial tissue was scaled (mm) two-dimensionally before and after endometrial biopsy grafting [35]. The

Downloaded from https://academic.oup.com/biolreprod/advance-article-abstract/doi/10.1093/biolre/ioy242/5181331 by EKU Libraries user on 14 November 2018

endometriotic implants (endometriotic lesions) were photographed on a Nikon D3100 DSLR camera.

2.1.3 Histological analysis of endometriotic tissue: Endometriotic lesions were preserved in paraffin blocks and sectioned (5μm) serially using microtome (RM2125 RTS, Leica Biosystem, Germany) as described earlier [36]. Sections were deparaffinized, stained with hematoxylin and 0.5% eosin, then imaged using an Inverted Phase Contrast Microscope (TS100-F, Nikon, Japan) and a 5.2 megapixels digital camera (DS-Fi2-U3, Nikon, Japan) [36;37].

2.1.4 Immunohistochemistry: Immunostaining was carried out as described [36]. Briefly, tissue sections of the endometriotic lesion (5.0 μm in size) were deparaffinized, and antigen retrieval was performed in sodium citrate buffer (10 mM, pH 6), followed by quenching of the endogenous peroxide activity using Bloxall (SP-6000, Vector Laboratories Inc., CA, USA). Tissue sections were blocked with 5.0% goat serum and subsequently incubated overnight at 4°C with 1/100 dilutions in 2.0% goat serum of the primary antibodies (Antibodies specific to Endoglin #3290S, E-cadherin #3195S, FAK #3285S, N-cadherin #14215S, and RHOC #3430S were purchased from CST, USA. Other antibodies specific to phosphorylated-E-cadherin #ab76319 and vimentin #SAB4503083 were from Abcam, UK and Sigma-Aldrich, India respectively) [36;38-44] or normal rabbit IgG isotype (negative control). Tissue sections were incubated with biotinylated secondary antibody and later with ABC reagent (PK-4001, Vector Laboratories Inc.) for 1 hr. The color was developed with the aid of 3, 3'-diaminobenzidine (DAB) peroxidase substrate (SK-4100, Vector Laboratories Inc.) for 1 min. and counter-stained with hematoxylin (51275, Sigma-Aldrich Inc.) for 2 min. Finally, sections were mounted using DPX and imaged using a microscope (CKX41 Trinocular with Cooled CCD Camera Model Q Imaging MP5.0-RTV-CLR-10-C from Olympus, Tokyo, Japan) [36]. The staining intensity of all

Downloaded from https://academic.oup.com/biolreprod/advance-article-abstract/doi/10.1093/biolre/ioy242/5181331 by EKU Libraries user on 14 November 2018

these proteins in the cystic, stromal, and glandular compartments were quantified by Image-Pro Plus 4.0 software (MD, USA), and the results were expressed as score/count [45]. Herein, the score/count for both 4X (total score) and 40X objective magnifications (total and cell specific score) of IHC images (Fig. S3 and S4) were analyzed. Total score was calculated from the entire tissues, and cell- or compartment-specific score was the average of scores calculated from at least 4 random regions of the same compartment.

2.1.5 Protein extract preparation from endometriotic lesions: The excised eutopic and ectopic endometrial tissues were rinsed with a buffer (pH7.4) containing 100mM KCl, 3mM NaCl, 3.5mM $MgCl_2$, 10mM Pipes, phosphatase inhibitor cocktail (P5726, Sigma-Aldrich Inc.), and protease inhibitor cocktail (S8830, Sigma-Aldrich Inc.) as previously described [36]. Tissue was homogenized, and unbroken tissue/cells, nuclear, and mitochondrial fractions were removed by centrifugation at 200, 1500, and 12000 x g (4°C) for 10 min. respectively, and the remaining supernatant was used as whole (cytosolic and membrane) protein extract and stored at −80°C for subsequent use [36].

2.2 Analytical techniques

2.2.1 SDS-PAGE and Immunoblotting: Quantification of the whole protein extract was done using a BCA Protein Assay Kit (23225, Thermo Fisher Scientific). Proteins (20μg) were denatured in Laemmli buffer [46] containing beta-mercaptoethanol in a 4:1 ratio and resolved on a 7.5-12 % SDS-PAGE at constant 100V using a Tetra Protean Cell Vertical electrophoretic system (Bio-Rad, Hercules, CA, USA). The SDS-PAGE-separated proteins were transferred onto a PVDF membrane (IPVH00010, Merck-Millipore, MA, USA) by electroblotting using the Towbin method [47].

Downloaded from https://academic.oup.com/biolreprod/advance-article-abstract/doi/10.1093/biolre/ioy242/5181331 by EKU Libraries user on 14 November 2018

The blotted membranes were blocked in 5.0% nonfat milk for 2.0 hr followed by incubation with respective primary antibodies in 2.0% nonfat milk (1:1000 dilutions), or for the antibodies against phosphorylated proteins, incubation in BSA. Membranes were incubated overnight at 4°C with respective antibodies (FAK, E-cadherin, N-cadherin and RHOC). Other primary antibodies include anti-ITGB3 (13166S), phospho-FAK (3283S), RHOA (2117P), phosphorylated-RAC1 (2461P), phospho-SMAD2/3 (9520S), SMAD2/3 (8685S), phosphorylated-p38MAPK (9211), p38MAPK (9212), phosphorylated-PTEN (9549S), and PTEN (9188S), obtained from CST, USA. Antibodies against phosphorylated-RHOA (sc32954) and PCNA (sc7907) were purchased from Santa Cruz Biotechnology, USA. Anti-ITGB8 (HPA027796) and vimentin (SAB4503083) were purchased from Sigma-Aldrich, Bangalore, India. Antibody against phosphorylated-E-cadherin (ab76319) was from Abcam, UK. Anti-RHOG (04-486) was from Merck-Millipore, Bangalore, India, and anti-RAC1 (PA1-091) was purchased from ThermoFisher Scientific, Bangalore, India) [37-40;42;44;48-57]. These membranes were subsequently incubated for 1.0 hr with peroxidase-conjugated secondary antibody anti-rabbit IgG-HRP, anti-goat IgG-HRP, or anti-mouse IgG-HRP in 1:3000 dilutions in 2.0% nonfat milk. Immuno-reactive bands were visualized with ECL substrate (WBKL0500, Merck-Millipore, MA, USA) according to the manufacturer's protocol using ChemiImager/ Documentation System (Image Quant LAS 4000, GE Life Science, PA, USA). Protein band intensity was analyzed using Total Lab Quant 1D software version 5.0 (Nonlinear Dynamics, Newcastle Upon Tyne, UK). The bands of SMAD2/3, phospho-E-cadherin, E-cadherin, phospho-PTEN, and PTEN were detected after membrane stripping (with 72° C warmed 5mM EDTA for 2.0 min., twice) followed by re-hybridizing to the same blot. Similarly, p-SMAD2/3, vimentin, phospho-P38 (MAPK), P-38 (MAPK), and N-cadherin were developed on the same

Downloaded from https://academic.oup.com/biolreprod/advance-article-abstract/doi/10.1093/biolre/ioy242/5181331 by EKU Libraries user on 14 November 2018

blot. ITGB8, ITGB3, p-FAK, and FAK were also developed on the same blot after stripping the probed blots.

2.2.2 Real-time PCR: Total RNA was extracted under RNase-free conditions from the endometriotic lesions and uteri of sham and TGF-B1 treated endometriosis and non-endometriosis mice using TRIzol reagent (Sigma-Aldrich, India). cDNA was synthesized from 1.0 µg RNA from individual mice (n = 3 from each group) using the SuperScript III cDNA synthesis kit (18080-126 400, ThermoFisher Scientific) as described previously [38]. Real-time PCR was performed with the PowerUp SYBR Green Master Mix (ThermoFisher Scientific) using the QuantStudio™ 3 real-time PCR system (Thermo Fisher Scientific) using standard cycle conditions: 95°C for 10 mins; 55 cycles of 95°C for 30 sec, 55°C for 30 sec, 72°C for 30 sec. The comparative C_T ($\Delta\Delta C_T$) method, as described earlier [58], was used to calculate relative gene expression levels between different samples based on the threshold cycles (*CTs*) value of each sample generated by the qPCR system. The fold change was determined with respect to the ΔC_T value of the corresponding target gene of PBS-treated eutopic endometrial tissues from the animal group without endometriosis. Briefly, C_T (threshold cycle) values of each target gene were first normalized to that of *b-actin* from the same sample (ΔC_T). Thereafter, the fold change was determined with respect to the ΔC_T value of the corresponding target gene from PBS-treated eutopic endometrial tissue from non-endometriosis animals using the formula $2^{-\Delta\Delta C_T}$. All qPCR experiments were done in triplicate and the results averaged and presented with mean and S.E.M. The primers used in qPCR are listed in Suppl. table-1.

2.2.3 17-beta-estradiol hormone estimation: 17-beta-estradiol levels were assayed using an ELISA kit (ADI-900-008, Enzo LifeSciences, Inc., NY, USA.) as per the manufacturer's instructions which have been validated in our previous study [54]. Protein extracts of

Downloaded from https://academic.oup.com/biolreprod/advance-article-abstract/doi/10.1093/biolre/ioy242/5181331 by EKU Libraries user on 14 November 2018

endometriotic lesions (40 µg) (n = 3 in each group) were used for this assay. The absorbance at 405 nm was read using a micro-plate reader (iMarkMicroplate Reader, BIO-RAD, USA). Absorbance values were plotted in a bar graph format against a standard (17-beta-estradiol; pg/ml). The concentration of 17-beta-estradiol was calculated according to the standard curve [54].

2.2.4 RAC1 activation assay: The RAC1 activity was assayed with RAC1 G-LISA kit (BK-128, Cytoskeleton, CO., USA.) and the reaction performed as previously described [38;54]. Briefly, 60 µg of protein extract from each sample was added to individual wells pre-coated with RAC1-GTP-binding protein, and subsequently incubated with 50 µl of anti-RAC1. The HRP conjugated antibody against anti-RAC1 (50 µl) was added and the color was developed using HRP detection reagent (50 µl). The optical density was recorded at 490 nm using a spectrophotometer**.**

2.2.5 FAK activity (Y-397) measurement by ELISA: FAK activation by phosphorylation at tyrosine-397 (Y-397) was quantified using a sandwich ELISA kit (DYC4528E, R&D Systems, Inc. MN, USA) as per (optimized) manufacturer's protocol [38]. The 96-well plate was coated with capture antibody and blocked with 1% BSA. 50 µg of protein extract from each sample was added to individual wells, and subsequently incubated with FAK-specific antibody (PTK2). The streptavidin-HRP conjugated antibody was added to develop the color in the presence of HRP substrate and absorbance was measured at 450 nm with correction of wavelength at 570 nm using a spectrophotometer (BioRadi MARK microplate reader, Laboratories, CA, USA).

2.3 Cell culture and *in vitro* techniques

2.3.1 Cell culture: Human endometriosis (ovary/benign cyst) stromal cell line HS.832(C).T (Cat no. CRL7566) [59] and transformed human endometrial stromal cells T-HES (Cat. No. CRL4003) derived from the stromal cells obtained from an adult women with non-malignant

Downloaded from https://academic.oup.com/biolreprod/advance-article-abstract/doi/10.1093/biolre/ioy242/5181331 by EKU Libraries user on 14 November 2018

myomas [60] were purchased from ATCC, USA. Both, HS.832(C).T and T-HES cells lines were maintained in advanced DMEM/F12 (12634010, ThermoFisher Scientific, Bangalore, India) supplemented with 10% FBS (10082-147, ThermoFisher Scientific) and 1.0% antimycotics and antibiotics mix (154240-016, ThermoFisher Scientific), and grown at 37°C and 5.0% CO_2 concentration under humid conditions. Insulin, Transferrin and Selenous (ITS) supplement (I3146-5ML, Sigma-Aldrich Inc.) was also added in the medium for T-HES cells to a concentration of 1.0%. Here, T-HES cells were used as non-endometriotic cells .[60]

2.3.2 *In vitro* scratch wound healing assay: Migration of HS.832(C).T and T-HES cells in response to TGF-B1 was assessed using an *in vitro* scratch wound healing assay (n = 3). Briefly, cells were seeded into 12-well culture plates at 70–80% confluency [61]. The wound was scratched in the middle of the well with a 10µl pipette tip and treated with human recombinant TGF-B1 (ab50036, Abcam, MA, USA.) at 5.0 or 10ng/ml concentrations for 24 hr. Wound closure photographs were captured using Nikon's Eclipse TS100 microscope equipped with a digital camera (Nikon DSFi2, Nikon DSU3, Nikon, Japan). The wound area was measured (ImageJ 1.46r software, NIH., USA) and the results expressed as percent wound closure compared to control.

2.3.3 Immunofluorescence and confocal imaging: Cells were fixed and permeabilized as described earlier [38], blocked with 5.0% BSA, and incubated with primary antibodies to integrin-beta3, E-cadherin, N-cadherin, vimentin, normal mouse IgG-Alexa Fluor 488 (sc516606, Santa Cruz Biotechnology, USA.) and normal Rabbit IgG (2729, CST, USA.). Other primary antibodies were RHOG (HPA039871, Sigma-Aldrich Inc.), cytokeratin-FITC (F3418, Sigma-Aldrich Inc.) [62], RAC1 (05-389-AF-488, Merck-Millipore, USA.) [63], and VAV (sc-132, Santa Cruz Biotechnology, USA) [54;64]. Finally, we incubated the cells with compatible

Downloaded from https://academic.oup.com/biolreprod/advance-article-abstract/doi/10.1093/biolre/ioy242/5181331 by EKU Libraries user on 14 November 2018

goat anti-rabbit (H+L) secondary antibody conjugated to Alexa Fluor (AF) 488 (A11034, Thermo Fisher Scientific) or AF647 (A-21245, Thermo Fisher Scientific), and goat anti-mouse IgG (H+L) secondary antibody (A11029, ThermoFisher Scientific), all at a dilution of 1:200. Normal rabbit IgG was used as the isotype control for ITGB3, E-cad, vimentin and RHOG, while normal mouse IgG conjugated with AF488 was used for N-cad and cytokeratin. The DAPI (1000ng/ml) and rhodamine-labeled Phalloidin (R415, ThermoFisher Scientific) (1/500 dilution) stains were used simultaneously for nuclear and cytoskeleton staining respectively. Cells were imaged using a Leica TCS SP5 Confocal Laser Scanning Microscope using the 63X objective magnification in oil medium, along with 2.4 X zoom (151X). In order to localize the specific proteins in the HS.832(C).T cells during the *in vitro* scratch wound healing assay, we mainly captured cells forming the migration waves and migrating at the edge of the scratch wound. The fluorescence intensity of HS.832(C).T cells was calculated using the ImageJ1.46r software (NIH) and represented by corrected total cell fluorescence (CTCF). The CTCF was calculated as Integrated Density - (Area of selected cell × Mean fluorescence of background readings), and averaged by the total number of cells analyzed (indicated in graphs) as described previously [65]. The average fluorescence intensity of cells was measured from at least five different microscopic fields. Colormap script, ImageJ plugin was used for automated co-localization quantification of two fluorescent signals overlay. This method specifically computes the correlation of intensities between pairs of individual pixels in two different channels (ITGB3 with RAC1, cytokeratin with vimentin, and N-cadherin with E-cadherin). Bar graph represents the mean correlation index (Icorr) ± SEM. Icorr (scale -1 to +1) indicates the fraction of positively correlated pixels in the image [66;67]. .

Downloaded from https://academic.oup.com/biolreprod/advance-article-abstract/doi/10.1093/biolre/ioy242/5181331 by EKU Libraries user on 14 November 2018

2.3.4 Transwell invasion assay: The invasive capabilities of HS.832(C).T and T-HES cells were assessed by an invasion assay using Boyden chambers (Costar Corp, Bethesda, MD) coated with matrigel (Becton Dickinson, Bethesda, MD) as described previously [68]. The upper chamber was first coated with 80 µl matrigel (1:5 matrigel and DMEM without phenol red) and incubated overnight at 37°C and 5.0% CO_2. Both cell lines were diluted to $5.0x10^4$ cells/ml in DMEM medium supplemented with 0.5% FBS. The upper chamber was filled with 250 µl of cell suspension, and the lower chamber with 750 µl of DMEM supplemented with 10% FBS (chemoattractant). Upper chambers were either supplemented with TGF-B1 (10 ng/ml) or left untreated as controls. After incubation, cells on the lower surface of the membrane were fixed and stained with 0.1% crystal violet (Sigma–Aldrich, Inc.). The membranes were photographed at 10X magnification, and the numbers of invading cells were counted in at least 10 different microscopic fields. The mean cell numbers and S.E.M were graphed in terms of fold change relative to the control HS.832(C).T group.

2.3.5 Invasion of 3D-spheroid-embedded HS.832(C).T and T-HES cells into matrigel: The invasion of HS.832(C).T and T-HES cells from embedded 3D-spheroids (formed by the hanging drop method) into the surrounding matrigel was investigated in the presence or absence of TGF-B1 for 48 hr as described previously [69]. In brief, 20 µl drops of both HS.832(C).T and T-HES cells (5000 cells/ml in complete DMEM medium) were spotted onto the inner side of the lid of a 90x15 mm Petri dish (64 drops/lid). The base of the Petri dish was filled with 5.0 ml sterile PBS to maintain humidity during incubation. After 2.0 min, the base was covered with the lid containing the cell-drops (spheroids), and incubated at 37°C in a CO_2 incubator for 48 hr. The spheroids were collected in a 5.0ml tube, mixed gently with matrigel diluted in 10% FBS

Downloaded from https://academic.oup.com/biolreprod/advance-article-abstract/doi/10.1093/biolre/ioy242/5181331 by EKU Libraries user on 14 November 2018

supplemented DMEM (1:3), then plated in 12-well culture plates at 10-15 spheroids per well. After 30 min, 2.0ml DMEM medium was added. At least three wells per experimental condition were either treated with 10 ng/ml of TGF-B1 or left untreated as controls. After 48 hr of incubation, images of wells were captured using Nikon's Eclipse TS100 microscope equipped with a digital camera (Nikon DSFi2, Nikon DSU3, Nikon, Japan) at 10X magnification. The area covered by cells that egressed from the spheroids into the surrounding matrigel matrix was measured in terms of the distance of each cell from the edge of 3D-spheroids using ImageJ 1.46r software (NIH, USA). The results were expressed as a percentage of the mean with S.E.M.

2.3.6 Colony formation assay: The HS.832(C).T and T-HES cells (500 cells per well) were cultured for 48 hr in a 6-well culture plate in the presence or absence of 5.0 or 10 ng/ml TGF-B1. The plate was then further incubated for 15 days with a medium change on every second day. Finally, the cells were fixed with 4.0% paraformaldehyde. The colonies were stained with crystal violet for 15 min. and washed under tap water. After air drying, the plate was scanned and images were analyzed using ImageJ1.46r software. The results were graphed in terms of mean colony number and S.E.M.

2.4 Statistical analyses: All analyses were performed using at least three independent animals per experimental condition and at least three independent sets of *in vitro* cell culture experiments. The average size of endometriotic lesions was presented as the mean ± S.E.M (standard error of the mean). For immunoblots, the densitometric value of each band was normalized to the corresponding B-ACTIN value, then averaged. ELISA values were also expressed as mean ± S.E.M. Statistical significance of respective *in vivo* and *in vitro* data sets was calculated by applying one-way ANOVA-tests followed by Bonferroni tests for the comparison of multiple groups, or unpaired two-tailed student's *t*-tests for comparisons between

Downloaded from https://academic.oup.com/biolreprod/advance-article-abstract/doi/10.1093/biolre/ioy242/5181331 by EKU Libraries user on 14 November 2018

only two groups. (* *p<0.05, ** (p <0.001), ***(p <0.0001, ns* p> 0.05). Herein, (a), (b), and (c) values represent comparisons between groups resulting in p-values <0.01; (a) compared TGF-B1-treated ectopic vs. eutopic endometrial tissues, (b) compared PBS-treated ectopic vs. eutopic endometrial tissues, and (c) compared the TGF-B1-treated eutopic endometrial tissue from endometriosis vs. non-endometriosis groups. The comparison (d) was also made between the PBS-treated eutopic endometrial tissues vs. non-endometriosis tissues from the endometriosis group.

3. Results

3.1. TGF-B1 potentiates endometriotic lesion development in a mouse model. We mimicked an elevated level of TGF-B1 by injecting a mouse model of endometriosis with recombinant active mTGF-B1 (14 ng/ml) to increase TGF-B1 concentration (gain of function) in the peritoneum, as described earlier [30;32;33]. We observed that TGF-B1-supplemented endometriotic ectopic implants in the peritoneal regions were hypertrophic compared to the PBS/sham control group (Fig. 1A-B).

Our histopathological observations by hematoxylin and eosin staining revealed that the peritoneal-implanted endometrial tissue of the PBS/control group had a significant presence of cysts with glandular epithelial mitosis and proliferation, macrophage infiltration, stromal proliferation, and mild fibrosis with increased numbers of stromal blood vessels (Fig. 1C). On the other hand, tissue from the TGF-B1-treated animal group displayed more cystic characteristics compared to the control/PBS animal group tissue. Although, we did not carry out quantitative analysis, but endometriotic lesions from the TGF-B1-supplemented animal groups appeared to have more mononuclear cell proliferation and stromal fibrosis (Fig. 1C). Overall, it appears that TGF-B1 induced more cellular proliferation with enhanced mononuclear

Downloaded from https://academic.oup.com/biolreprod/advance-article-abstract/doi/10.1093/biolre/ioy242/5181331 by EKU Libraries user on 14 November 2018

infiltrations (confirmed by PCNA and P38 MAPK expression in Fig. S1A-B. The characteristics of these endometriotic lesions recapitulate the endometriosis model described earlier.

3.2 TGF-B1-induced progression of endometriotic lesions is independent of 17-beta-estradiol (E2) signaling. We used competitive ELISA to determine the 17-beta-estradiol (E2) level in endometriotic lesions from peritoneal regions. We found that the E2 level was unaffected in the TGF-B1-supplemented group when compared to the PBS/sham control group; the concentration was nearly 1000 pg/ml (in 40 microgram protein extract) in both groups (Fig. 1D). These observations suggest that E2 level is independent of TGF-B1 in endometriosis in this autologous endometriosis mouse model.

3.3 Activation of the TGF-B1 signaling cascade in the TGF-B1-supplemented endometriosis mouse model. We observed that the TGF-B1-treated animals with endometriosis showed aggravation of lesions (ectopically implanted eutopic endometrial tissue) at the peritoneal site (Fig. 1A-C). Therefore, we first investigated changes in SMAD2/3 and phospho-SMAD2/3 (Serine 465/467 and Serine 423/425 respectively) expression levels in response to TGF-B1 in ectopic (endometriotic animals only) and eutopic endometrial tissues (endometriotic and non-endometriotic animals) (Fig. 1F). Interestingly, our results showed that TGF-B1 supplementation increased SMAD2/3 expression significantly in all the groups. However, SMAD3 expression was not elevated any further in the eutopic tissues of animals with endometriosis even after TGF-B1 supplementation. The level of active phosphorylated SMAD2/3 increased significantly only in the TGF-B1-treated endometriotic lesions (ectopic endometrium) in comparison to the PBS-treated lesions (Fig. 1F). Indeed, after TGF-B1 exposure, SMAD2 expression increased significantly in the eutopic and ectopic endometrial tissues in the animals with endometriosis

Downloaded from https://academic.oup.com/biolreprod/advance-article-abstract/doi/10.1093/biolre/ioy242/5181331 by EKU Libraries user on 14 November 2018

compared to the animals without endometriosis. We observed the same pattern of SMAD3 expression in the ectopic endometrial tissue of animals with endometriosis and eutopic endometrial tissue of animals without endometriosis (Fig. 1F). Based on q-PCR data, we observed TGF-B1-dependent increases in *Smad2* transcript levels in the eutopic and ectopic endometrial tissues of animals either with or without endometriosis, but the effect was greater in the endometriotic tissue (Fig. 1G). Similarly, TGF-B1 increased *Smad3* transcript level, but not in the ectopic endometrial tissues from PBS-treated animals with endometriosis. However, the effect of TGF-B1 on *Smad3* was stronger in the ectopic endometrial tissues of animals with endometriosis than in the eutopic endometrial tissue of animals either with or without endometriosis (Fig. 1H).

Endoglin, an auxiliary receptor of TGF-B1, is a member of the TGF-B1 superfamily. It is an established biochemical marker of angiogenesis, and is present in the stromal and epithelial cells of the endometrium [36]. We studied the immunolocalization of endoglin in endometriotic lesions from the pelvic regions of TGF-B1-treated animals with endometriosis and from a corresponding PBS/control group (Fig. 1E). Higher endoglin expression was seen only in the cystic and stromal regions of endometriotic lesions in TGF-B1-treated animal groups and not in PBS-treated animals. Endoglin expression was not detected in the glandular region (Fig. 1E). The score/count calculation suggested that the only significant difference was between the cystic regions of endometriotic lesions from TGF-B1 treated animals and the control group (Fig. S3 A-C). There was no difference in *Endoglin* transcript levels between the ectopic endometrial tissue of TGF-B1-treated and PBS/control animal groups (Fig. S2A). However, TGF-B1 treatment induced a higher level of *Endoglin* transcript in eutopic endometrial tissue from both endometriosis and non-endometriosis groups (Fig. S2A).

Downloaded from https://academic.oup.com/biolreprod/advance-article-abstract/doi/10.1093/biolre/ioy242/5181331 by EKU Libraries user on 14 November 2018

3.4 Expression of endometriosis-associated biomarkers in TGF-B1-augmented endometriosis. Extensive cell proliferation is required for the growth and development of ectopic endometriotic lesions. To confirm the TGF-B1-mediated cell proliferative response, we looked into the expression pattern of cell proliferative biochemical markers, proliferating cell nuclear antigen (PCNA) and P38 MAPK [70], in the endometriosis-like lesions in the peritoneal region of the mouse model. Cell proliferation was assessed by immunoblotting for PCNA and P38 MAPK in the eutopic and ectopic endometrium tissues from the animal groups with endometriosis (sham and TGF-B1-treated groups) and without endometriosis (Fig. S1A-B). After TGF-B1 supplementation, we observed increased expression of PCNA in endometriotic lesions and eutopic endometrial tissues from animal groups with endometriosis versus PBS-treated animal groups (Fig. S1A and D). TGF-B1 treatment had no significant or specific effect on P38MAPK expression in the ectopic or eutopic endometrial tissues from animals with or without endometriosis (Fig. S1B and E). The expression pattern of the phosphorylated (Threonine 180/ Tyrosine 182) form of P38MAPK (phospho-P38MAPK) was similar to that of P38MAPK (Fig. S1B). However, phospho-P38MAPK levels slightly declined in the eutopic endometrial tissue of the TGF-B1-treated animal group with endometriosis compared to PBS-treated animal group with endometriosis (Fig. S1B and E)

We also analyzed the expression levels of PTEN, a known tumor suppressor reported to be reduced in endometriosis [71], and phospho-PTEN (Serine 380/Threonine382/383). Here, we found that the basal protein expression level of total PTEN was almost the same in all groups (Fig. S1C and F). Importantly, the phosphorylation of PTEN was significantly suppressed in the TGF-B1-supplemented compared to control/sham-treated ectopic lesions of the animal group

Downloaded from https://academic.oup.com/biolreprod/advance-article-abstract/doi/10.1093/biolre/ioy242/5181331 by EKU Libraries user on 14 November 2018

with endometriosis (Fig. S1C and F). The eutopic endometrial tissues from TGF-B1- and PBS-treated animal groups with endometriosis, and from TGF-B1-treated animals without endometriosis, displayed higher phosphorylated-PTEN levels compared to ectopic endometrial tissue from the TGF-B1-treated group (Fig. S1C and F). The basal level of *Pten* transcript was decreased in the ectopic and eutopic endometrial tissues of the animal group with endometriosis relative to the animal group without endometriosis (Fig. S1G). Therefore, we confirmed the action of externally supplemented recombinant active TGF-B1 on the known endometriosis biomarkers/signaling molecules.

3.5 Expression of integrins and FAK was enhanced in the endometrial tissue of TGF-B1-supplemented animals. Aberrant expression of integrins and FAK have already been reported in endometriosis [25;72]. Hence, to understand how adhesion molecules affect ectopic endometrial tissue growth in response to TGF-B1, we assessed the expression patterns of members of the integrin-signaling pathway in ectopic endometriotic lesions and eutopic endometrium. Immunoblotting analysis showed a significant upregulation of integrin beta3 (ITGB3) in both ectopic endometriotic lesions from the peritoneal region and eutopic endometrium from the endometriosis group (Fig. 2A). Importantly, TGF-B1 elevated the expression of ITGB3 in ectopic and eutopic endometrial tissues in the endometriosis groups (Fig. 2A). Conversely, TGF-B1 suppressed the expression of ITGB3 in the eutopic endometrium of the animal group without endometriosis (Fig. 2A). Interestingly, *Itgb3* transcript levels were also high in the ectopic endometrial tissue of the animal group treated with TGF-B1 (Fig. S2A). However, while the expression of *Itgb3* did not differ between the eutopic endometrial tissue from the PBS- versus TGF-B1-treated animal groups with endometriosis (Fig. S2B), it was lower

Downloaded from https://academic.oup.com/biolreprod/advance-article-abstract/doi/10.1093/biolre/ioy242/5181331 by EKU Libraries user on 14 November 2018

in the eutopic endometrial tissue of the non-endometriosis group compared to the endometriosis group (Fig. S2B).

In the case of integrin beta8 (ITGB8), TGF-B1 significantly enhanced the protein expression only in the endometriotic lesions (ectopic endometrium), but not in the eutopic endometrium, of animal groups with or without endometriosis (Fig. 2B). Similarly, the transcript level of *Itgb8* was increased significantly in the ectopic lesions of the TGF-B1 treated animal group compared to the PBS/control ectopic lesions (Fig. S2C). The eutopic tissue from animals with endometriosis treated with either TGF-B1 or PBS exhibited lower levels of *Itgb8* expression; these levels were further decreased in the eutopic endometrial tissue of the animal group without endometriosis (Fig. S2C).

Subsequently, we checked the expression level of integrin signaling associated molecule, FAK (total and phosphorylated forms), in the endometriotic lesions. Interestingly, after TGF-B1 treatment, the expression of total FAK was significantly elevated in the ectopic endometriotic lesions (Fig. 2C) compared to the eutopic tissues from both endometriosis and non-endometriosis groups (Fig. 2C). Further, the FAK activity (phosphorylation; Tyrosine-397) was approximately 4-fold higher in the endometriotic lesions of animal groups treated with TGF-B1 relative to control-treated animal groups (Fig. 2F).

Additionally, we extended our study by localizing FAK in the ectopic endometrial tissues of animal groups with endometriosis (Fig. 2D and E). FAK exhibited milder expression in the glandular region and stromal region of the endometriotic lesions in sham-treated animal groups. On the other hand, intra-peritoneal administration of TGF-B1 significantly increased the immunostaining score of FAK in the cystic area and decreased in the glands of the ectopic endometrial tissue (Fig. 2D and E) (Fig. S3 D-F).

Downloaded from https://academic.oup.com/biolreprod/advance-article-abstract/doi/10.1093/biolre/ioy242/5181331 by EKU Libraries user on 14 November 2018

3.6 TGF-B1 induces expression of Epithelial-Mesenchymal Transition (EMT) biomarkers in peritoneal endometriotic lesions. Altered expression levels of N-cadherin and E-cadherin are reported to be involved in the ectopic attachment of endometrial cells, thus giving rise to endometriosis [73;74]. We evaluated the expression level of these cadherins in response to TGF-B1 by immunoblotting of protein extracts derived from the peritoneal endometriotic lesions and eutopic endometrium of both the endometriosis and non-endometriosis animal groups (Fig. 3A). Importantly, high levels of total E-cadherin were observed in the eutopic endometrial tissue of animals without endometriosis, but significantly reduced in endometriotic lesions from the peritoneal region in the animal groups treated with TGF-B1 (Fig. 3A and B). However, its phosphorylated form (Serine 838/840) was increased in the ectopic endometrial tissue of TGF-B1-supplemented animal groups (Fig. 3A and B). In the eutopic endometrium of animals without endometriosis, TGF-B1 supplementation significantly reduced the total E-cadherin level, but increased the levels of its phosphorylated form (Fig. 3A and B). On the other hand, in the eutopic endometrium of animals with endometriosis, total E-cadherin was increased in the presence of the TGF-B1, but the phosphorylated form of E-cadherin was not affected (Fig. 3A and B).

Remarkably, N-cadherin expression was elevated only in the ectopic endometriotic lesions from endometriosis animal group after TGF-B1 treatment, but not after PBS treatment (Fig. 3A and C). TGF-B1 supplementation exerted an additive effect (~4-fold higher) on N-cadherin expression in the endometrial tissue (both ectopic and eutopic) of animals with endometriosis compared to animals without endometriosis (Fig. 3A and C).

The expression pattern of vimentin was similar to E-cadherin; upon TGF-B1 supplementation, vimentin expression increased in the ectopic endometrial tissue of animals with

Downloaded from https://academic.oup.com/biolreprod/advance-article-abstract/doi/10.1093/biolre/ioy242/5181331 by EKU Libraries user on 14 November 2018

endometriosis (Fig. 3A and D) relative to its basal level in the eutopic endometrial tissues of animals with or without endometriosis (Fig. 3A and D).

Thereafter, we performed immunolocalization and quantification of E-cadherin, N-cadherin, and vimentin expression (Fig. 3E-I and Fig. S4). In the endometriotic lesions of the sham group, E-cadherin was localized to both stromal and cystic regions (Fig. 3F). In PBS-treated tissues, E-cadherin was also visibly expressed in both stromal cells and cystic regions. Although E-cadherin was present in both stromal cells and cystic regions of the endometrial tissues of TGF-B1-treated animals, their expression levels were significantly low (Fig. 3E-F and Fig. S4A-C). The staining of phospho-E-cadherin was observed in the stromal and cystic regions of ectopic endometrial tissue from animal groups with endometriosis after PBS and TGF-B1 treatment. Immunostaining score analysis showed that after TGF-B1 treatment, phospho-E-cadherin was reduced in the stromal region, but increased in the cystic region (Fig. 3E and G and Fig. S4 D-F). N-cadherin was seen primarily in stromal cells and cystic areas of ectopic endometrial tissue from peritoneal endometriotic lesions, and was significantly increased (score/count) in TGF-B1-treated animal groups (Fig. 3E and H and Fig. S4 G-I).

Further, we assayed vimentin localization in the ectopic endometrial tissues from endometriotic lesions that developed in response to TGF-B1 and PBS supplementation in the mouse model. Vimentin is a component of the cytoskeleton that is involved in the arrangement of cell organelles, and is a marker of mesenchymal cells. Immunolocalization of vimentin showed its ubiquitous expression in the endometriotic lesions from the endometriosis group (Fig. 3E and I). In response to TGF-B1, the expression of vimentin was prominent in both stromal and cystic compartments when compared to the PBS-treated animal group (Fig. 3E and I and Fig. S4 J-L). Overall, immunoblotting and immunolocalization studies showed that TGF-B1 promotes

Downloaded from https://academic.oup.com/biolreprod/advance-article-abstract/doi/10.1093/biolre/ioy242/5181331 by EKU Libraries user on 14 November 2018

EMT in the development of ectopic lesions. E-cadherin (total and phospho forms), N-cadherin, and vimentin were not detectable in the glandular regions. Normal rabbit IgG was used as control and did not show any false positives resulting from cross-reactive immunostaining (lower panels).

3.7 TGF-B1 drives expression of N-cadherin and vimentin, suppresses cytokeratin and E-cadherin, and enhances the migratory potential of human ovarian endometriotic cells (HS.832(C).T). We assessed the expression levels of E-cadherin, N-cadherin, and vimentin, in response to TGF-B1 by immunoblotting (Fig. 4A-C). In the presence of TGF-B1, total E-cadherin and phosphorylated-E-cadherin were downregulated in the endometriotic cells (Fig. 4A), while N-cadherin and vimentin were induced (Fig. 4B and C).

Subsequently, we examined E-cadherin and N-cadherin co-localization in human ovarian endometriotic cells (HS.832(C).T). Both cadherins were co-localized in control- and TGF-B1-treated groups, predominantly in the membrane compartment (Fig. 4D). We then assessed cytokeratin and vimentin co-localization in HS.832(C).T cells after TGF-B1 treatment (Fig. 4E). The epithelial cell biomarker, cytokeratin, was present in the control group, but was not detectable in the TGF-B1 group (Fig. 4 E). Our confocal microscopy-based observations, followed by fluorescence intensity quantification in terms of corrected total cell fluorescence (CTCF), revealed that the intensities of N-cadherin and vimentin staining increased significantly after TGF-B1 treatment, while cytokeratin fluorescence was reduced (Fig. 4F). Surprisingly, the intensity of E-cadherin staining remained unchanged in these experiments.

Further, we wanted to investigate the effect of TGF-B1 on N-cadherin expression in migratory HS.832(C).T cells. In order to model migratory endometriotic cells, we used an *in vitro* scratch wound healing assay. We performed the assay in HS.832(C).T cells in either the

Downloaded from https://academic.oup.com/biolreprod/advance-article-abstract/doi/10.1093/biolre/ioy242/5181331 by EKU Libraries user on 14 November 2018

presence or the absence of TGF-B1 (10ng/ml), for 24 hours in a 12-well culture plate (Fig. 4L and M). First, we checked the effect of TGF-B1 on migration of these cells and found that it accelerated cell migration leading to wound closure (Fig. 4L and M). Next, we examined N-cadherin expression in the migratory HS.832(C).T cells (specifically cells present at the edge of the wound). We found that TGF-B1 (10ng/ml)—increased the migration capabilities of HS.832(C).T cells by increasing the expression of N-cadherin in the cells (Fig. 4 L and M indicated by red square). These observations suggest that EMT was enhanced in the presence of TGF-B1, mainly in the migratory endometriotic cells.

3.8 TGF-B1 enhanced the expression of ITGB3 and RAC1 in the human ovarian endometriotic cells (HS.832(C).T). Using confocal laser scanning microscopy, we further extended our localization study to examine the response of ITGB3, VAV, RAC1, and RHOG to TGF-B1 treatment in the HS.832(C).T cell line. We performed immunofluorescence to determine co-localization of ITGB3 and RAC1 in human ovarian endometriotic cells. RAC1 was present throughout the cells in control groups (Fig. 4H). By employing CTCF analysis with the ImageJ software (NIH), we observed that TGF-B1 treatment promoted peripheral expression of RAC1 in the HS.832(C).T cell line (Fig. 4H and K). ITGB3 was prominently expressed in the cell membrane in both control- and TGF-B1-treated groups, but TGF-B1 treatment further enhanced its expression (Fig. 4H and K). ITGB3 and RAC1 co-localization in the HS.832(C).T cells was also enhanced by TGF-B1 treatment (Icorr. 0.82±0.01) than untreated (0.66±0.01) (Fig. 4G).

Subsequently, we examined the localization pattern of the RAC1 activator, VAV. VAV was present at low levels in the HS.832(C).T cell line in control group; however, its expression

Downloaded from https://academic.oup.com/biolreprod/advance-article-abstract/doi/10.1093/biolre/ioy242/5181331 by EKU Libraries user on 14 November 2018

was enhanced upon TGF-B1 treatment (Fig. 4I and K). We reported earlier that RHOG can activate RAC1 [37]; therefore, we analyzed RHOG expression in the HS.832(C).T cell lines. Similar to VAV, RHOG exhibited low expression in the control group of cells, but its expression was augmented in response to TGF-B1 treatment (Fig. 4 J and K). The respective antibody isotype controls (rabbit or mouse IgG) did not yield any detectable fluorescence (Fig. 4H, I and J).

3.9 TGF-B1 accelerated wound-healing by upregulating expression of RAC1 and VAV in human ovarian endometriotic cells. Herein, we noticed that TGF-B1 enhanced the migration of HS.832(C).T cells; the wound area was completely covered in 24 hours (Fig. 4L). Further, the expression of RAC1 and VAV was localized to the HS.832(C).T cells present at the edges of the wound created by scratching the monolayer of cells (Fig. 4L indicated by asterisk). Based on confocal imaging and fluorescence intensity profiling, we found that in the control group, low expression of VAV and RAC1 was observed mainly in the nuclear and cytosolic regions (Fig. 4N and O). Phalloidin-stained cytoskeletons in the cells reflected the formation of migratory waves at the edge of the scratched wound (Fig. 4 M, N and O).

In parallel to the endometriotic (HS.832(C).T) cells, we also examined the migration of T-HES cells, a model of endometrial cells from an endometriosis-free source, in response to TGF-B1 (Fig. 6A-B). Interestingly, we found that the basal migration capacities of both cell lines were similar at 24 hr. However, the migration capacity of HS.832(C).T cells was further increased significantly with 10 ng/ml TGF-B1 treatment, and to a greater degree than that of the T-HES cells (Fig. 6A-B). The 10 ng/ml dose of TGF-B1 can also trigger 62% more migration of non-endometriotic stromal cells than the 5 ng/ml TGF-B treated group (Fig. 6A-B).

Downloaded from https://academic.oup.com/biolreprod/advance-article-abstract/doi/10.1093/biolre/ioy242/5181331 by EKU Libraries user on 14 November 2018

3.10 TGF-B1 promotes the activity and expression of RHOGTPases in ectopic endometrial tissues. RHOGTPases are crucial for cell migration, cytoskeleton dynamics, adhesion, and inflammation. Increased expression of RHOA and RHOC are also reported to assist the migration of endometrial cells during endometriosis [61;75;76]. We wanted to determine if TGF-B1 induces cell migration in the endometriotic lesions through the involvement of RHOGTPases (Fig. 5). Herein, our immunoblotting data revealed that the levels of total RHOA and its Serine-188 phosphorylated form were slightly increased in the ectopic endometrial tissue of animals treated with TGF-B1 compared to the eutopic endometrial tissues of animals either with or without endometriosis (Fig. 5A and E).

Thereafter, we found that RAC1 expression was significantly higher in the endometriotic lesions in TGF-B1-treated animals compared to PBS-treated animals (Fig. 5B and F). However, in the eutopic endometrial tissues of animal with or without endometriosis, TGF-B1 treatment had no significant effect on RAC1 expression, but did significantly increase RAC1 phosphorylation at Serine-71 in the endometriotic lesions (Fig. 5B and F).

Having observed this differential expression pattern of RAC1 in endometriosis, we looked at the level of active RAC1 (RAC1-GTP bound form) (Fig. 5G). We found that RAC1 activity was increased in the endometriotic lesions of TGF-B1-treated animals and in eutopic endometrial tissue of TGF-B1-treated animal without endometriosis, compared to their respective PBS-treated control groups (Fig. 5G). In contrast, the level of active RAC1 was significantly decreased in the eutopic endometrial tissue of endometriotic animals treated with TGF-B1.

Then, we checked the expression level of RHOC and found it present in the tissues of all groups (Fig. 5C). Importantly, TGF-B1 significantly induced the expression of RHOC in the ectopic lesions, but not in the eutopic endometrial tissues of animals with or without

Downloaded from https://academic.oup.com/biolreprod/advance-article-abstract/doi/10.1093/biolre/ioy242/5181331 by EKU Libraries user on 14 November 2018

endometriosis (Fig. 5C and H). The transcript level of *Rhoc* was also significantly elevated in the endometrial tissue of animals with endometriosis in comparison to endometrial tissues of animals without endometriosis (Fig. S2D).

Next, we assessed RHOC localization by analyzing the immunostaining score analysis using Image Pro Plus 4.0 software (Fig. 5I and J). Except the glandular region, RHOC was expressed in all cell types of the ectopic endometrial lesions from animals treated with PBS. However, the expression was increased in endometriotic tissues (sections) from animals treated with TGF-B1 (Fig. 5I and J). In the control (PBS) treated animal group, RHOC showed more intense localization in the stromal cells and cystic regions of endometrial tissue (Fig. 5I). After immunostaining score analysis, we found that RHOC expression was significantly increased in both stromal cells and cystic regions, but not detectable in the glandular region of endometrial tissue from animals treated with TGF-B1 (Fig. 5I-Jand Fig. S3 G-I).

The expression of RHOG was also analyzed in a similar manner (Fig. 5D and K). RHOG expression was increased in the ectopic endometrial tissues of TGF-B1-treated animals compared to PBS-treated animals (Fig. 5D and K). However, the expression level of RHOG was lower in the ectopic compared to eutopic endometrial tissues of animals with endometriosis treated with either TGF-B1 or PBS (Fig. 5D and K). Surprisingly, the ectopic endometrial tissues of animals with endometriosis and eutopic endometrial tissue of animals without endometriosis both demonstrated TGF-B1-dependent elevation of RHOG expression (Fig. 5D and K).

Interestingly, *Rhog* transcript levels were increased by TGF-B1 treatment in ectopic and eutopic endometrial tissues of animals with or without endometriosis (Fig. S2E). Nevertheless, the magnitude of *Rhog* expression in the ectopic endometrial tissue was low (Fig. S2E).

Downloaded from https://academic.oup.com/biolreprod/advance-article-abstract/doi/10.1093/biolre/ioy242/5181331 by EKU Libraries user on 14 November 2018

3.11 TGF-B1 promotes human ovarian endometriotic cell invasion. The other important feature of the endometriotic cell is its invasive capacity [4;77]. We performed transwell invasion assays using endometriotic cells (HS.832(C).T cells) and non-endometriotic stromal cells (T-HES cells) in response to TGF-B1 treatment (10 ng/ml) for 48 hr. We found that the basal invasive potential of HS.832(C).T cells was significantly higher than the T-HES cells (Fig. 6C-D). TGF-B1 enhanced the invasion of only HS.832(C).T cells across the matrigel; moreover, the HS.832(C).T cell line had a much greater response to TGF-B1 treatment than the T-HES cells (nearly 3-fold versus 1-fold increase in invasive capacity)(Fig. 6C-D).

3.12 TGF-B1 promotes HS.832(C).T and T-HES cells invasion in 3D-spheroid culture. We also investigated the invasion of HS.832(C).T and T-HES cells, from 3D-spheroids in which they were embedded, into the surrounding matrigel (Fig. 6E-F). After a 48-hour incubation in the presence or absence of TGF-B1, we measured the area covered by the cells that had egressed from the spheroids into the surrounding matrigel. Egression of both HS.832(C).T and T-HES cells was increased by TGF-B1 treatment in comparison to untreated controls (Fig. 6E-F). Although the basal invasion or spreading potential of the CRL755 cells into the matrigel was higher than the T-HES cells, HS.832(C).T cell line-spheroids showed a greater response than the T-HES cells to TGF-B1 treatment (10ng/ml) (Fig. 6E-F).

3.13 TGF-B1 enhanced the colony forming potential of HS.832(C).T and T-HES cells. In endometriosis, ectopic colonization by endometrial cells is an important feature for the establishment of lesions. Previous reports have documented colonization and embedment of endometriotic cells (endometrial glands) within the intestinal wall [78;79]. Using an *in vitro*

Downloaded from https://academic.oup.com/biolreprod/advance-article-abstract/doi/10.1093/biolre/ioy242/5181331 by EKU Libraries user on 14 November 2018

clonogenic assay, we investigated the TGF-B1-modulated colony forming potential of HS.832(C).T and T-HES cells (Fig. 6G-H). We observed that untreated T-HES cells formed smaller colonies than HS.832(C).T cells. However, TGF-B1 treatment (10ng/ml) promoted the colonization potential of both types of cells (Fig. 6G-H).

4. Discussion

Endometriosis is characterized by severe inflammation and pelvic pain in women of reproductive age. Cytokines, chemokines, proteases, and growth factors have been found to be involved in the pathogenesis of endometriosis [23;80;80]. Pro-inflammatory cytokines, such as TGF-B1, can promote the migration of endometrial cells in human endometriosis [81]. Further, abnormally elevated levels of TGF-B1 in the peritoneal fluid, endometriotic tissue, and serum of endometriosis patients, suggest that TGF-B1 could be an important contributing factor in the development of endometriosis [9;82;82;83]. We speculated that the exposure of floating endometrial cells/tissues to high TGF-B1 in the peritoneal region potentially impacts the development of endometriosis. Such an exposure may trigger various signaling pathways and cellular processes like adhesion, migration, EMT, proliferation, invasion, and colonization to favor the ectopic growth of these cells.

We used a recognized and validated mouse model of endometriosis [31;84] where we surgically auto-transplanted (sutured) endometrial tissue to the peritoneal wall of the same animal as described earlier [31;32], and further validated the model biochemically and histologically. In parallel, we supplemented the animals (with or without endometriosis) with recombinant TGF-B1 to dissect the specific effect of TGF-B1 in the development of endometriosis. Histologically, TGF-B1 induced the development of endometriotic lesions within the mouse models; these resembled human endometriotic lesions and exhibited cyst-like

Downloaded from https://academic.oup.com/biolreprod/advance-article-abstract/doi/10.1093/biolre/ioy242/5181331 by EKU Libraries user on 14 November 2018

structures. The endometriotic tissue displayed epithelium-lined structures consisting of stromal cells and endometrial glands. Morphologically, TGF-B1 administration led to increased growth of the endometriotic lesions (size), and excessive cell proliferation in the endometriotic lesions of pelvic endometriosis, which was further evidenced by PCNA expression levels. Endometriosis is a steroid hormone-dependent disorder in which 17-beta-estradiol participates in the endometrial cell invasion and proliferation [1]. Importantly, we observed that TGF-B1 mediated excessive growth of endometriotic lesions, independent of 17-beta-estradiol in this autologous endometriosis mouse model.

Canonically, TGF-B1 transduces signals via SMAD2/3 activation in the endometrium [51;53]. Interestingly, the action of TGF-B1 was profoundly associated with its classical signaling molecule SMAD2/3 in the ectopic endometrial tissue, but not in the eutopic endometrial tissue from animal groups with or without endometriosis. Concomitant activation of SMAD2/3 were observed in response to TGF-B1 in the ectopic endometriotic lesions compared to the eutopic endometrial tissues, which overall, may favor the pathogenesis of endometriosis.

This particular action of TGF-B1 is supported by our analysis of endometriosis-associated biomarkers such as P38MAPK, RHOC, and RHOA in the endometriotic lesions of the mouse model of endometriosis. These molecules were significantly elevated in response to TGF-B1 supplementation; moreover, both RHOC transcript and protein expression were enhanced by TGF-B1 in the endometriosis cases (ectopic and eutopic endometrial tissues). We also found that TGF-B1 increased phosphorylation of RHOA in the ectopic endometrial tissue, an event associated with endometriosis development. P38MAPK is a known molecular target in endometriosis [70], previously shown to be activated by TGF-B1 [85]. In endometriosis, P38MAPK might promote pro-inflammatory cytokines and proteolytic factors as reported earlier

Downloaded from https://academic.oup.com/biolreprod/advance-article-abstract/doi/10.1093/biolre/ioy242/5181331 by EKU Libraries user on 14 November 2018

[70]. Interestingly, we also found that TGF-B1 activates P38MAPK in the ectopic endometrial tissue under the endometriotic condition, but the inverse action of TGF-B1 on P38MAPK was seen in the corresponding eutopic endometrial tissue; hence, the action of TGF-B1 in the endometrial tissue seems to be specific to disease state. Furthermore, in response to TGF-B1 supplementation, known biomarkers of endometriosis and TGF-B1 downstream target molecules such as endoglin (CD105) were enhanced and localized predominantly in the epithelial and stromal cells. On the whole, our endometriosis experimental model replicated the biochemical parameters of human endometriosis.

Further, elevated expression levels of PCNA protein and mRNA in ectopic lesions and eutopic endometrial tissue confirmed TGF-B1-induced growth in endometriosis. In contrast, the lower expression levels of *Pten* (tumor suppressor gene) and phosphorylated PTEN demonstrate the tumor-promoting behavior of TGF-B1 in the cysts of ectopic endometriotic lesions, but not in the eutopic endometrium, of the mouse models either with or without endometriosis. This is consistent with mutation or loss-of-function of *PTEN* being associated with a high risk of endometriosis [86], since PTEN controls cell-survival, growth and proliferation [87]. PTEN is stabilized by its phosphorylation *in vivo* [88], and we observed low levels of phosphorylated-PTEN. Therefore, the reduced level of phosphorylated-PTEN correlates with cell growth enhancement and ectopic endometrial tissue proliferation in response to TGF-B1.

Next, we wanted to understand the signaling pathways that might be associated with the pathophysiology resulting from the abnormal presence (upregulation) of TGF-B1 in the endometrium, endometriotic lesions, and peritoneal fluid [9]. In endometriosis, adhesion molecules affect the adhesiveness of floating endometrial cells [89]. Specifically, cadherins and integrins are associated with endometriosis [23]. However, the regulation of adhesion molecules

Downloaded from https://academic.oup.com/biolreprod/advance-article-abstract/doi/10.1093/biolre/ioy242/5181331 by EKU Libraries user on 14 November 2018

in endometriosis remained poorly understood. Interestingly, in the present work, we observed that TGF-B1 drove ITGB3 and ITGB8 expression at both the protein and mRNA level, as well as expression of the downstream signaling intermediate, FAK, in endometriotic lesions from the pelvic regions of animals with endometriosis. However, ITGB8 and FAK, but not ITGB3, showed basal levels of expression in the eutopic endometrial tissues from animals with or without endometriosis. This implies that TGF-B1 positively affects the ITGB8 and FAK expression under the endometriosis condition. ITGB3 expression was greatly affected by TGF-B1 in the eutopic and ectopic endometrial tissues of animals with endometriosis. FAK was also more prominent in the ectopic lesions after TGF-B1 supplementation. FAK has already been reported to participate in the pathogenesis of endometriosis [90]; therefore, its upregulation by TGF-B1 substantiates the conjecture that a TGF-B1-Integrin-FAK signaling axis might be operational in pelvic area endometriosis.

In order to obtain a suitable ectopic site for successful attachment and growth, the floating endometrial tissues undergo EMT and cell-migration [81]. TGF-B1 is a well-known regulator of EMT that upregulates N-cadherin and vimentin, but suppresses E-cadherin expression [41;91]. Herein, we report that the presence of TGF-B1 suppresses epithelial cell marker (E-cadherin) expression in the endometriotic lesions of animals either with or without endometriosis, to a greater extent than in the eutopic endometrial tissues of these animals. Surprisingly, in endometriosis, TGF-B1 seems to be an inhibitor of total E-cadherin, but a promoter of E-cadherin phosphorylation. This suggests that TGF-B1 prevents the interaction of E-cadherin with beta-catenin by enhancing phosphorylation of E-cadherin at its Threonine-790 residue in the endometriotic lesions as reported earlier [92]. In endometriotic lesions, E-cadherin was present in the glandular regions with the sham treatment, but shifted to the stromal cells

Downloaded from https://academic.oup.com/biolreprod/advance-article-abstract/doi/10.1093/biolre/ioy242/5181331 by EKU Libraries user on 14 November 2018

region and cystic fluid in response to TGF-B1. This indicates a shift of E-cadherin to its phosphorylated state. Notably, endometriotic lesions from animals supplemented with TGF-B1 exhibited higher levels of N-cadherin, which indicates epithelial to mesenchymal transition [81]. We further confirmed TGF-B1-mediated EMT in human ovarian endometriotic cells (HS.832(C).T) by confocal-based immunofluorescence studies of EMT markers such as E-cadherin, cytokeratin, N-cadherin, and vimentin. TGF-B1 promoted N-cadherin and vimentin expression, but suppressed cytokeratin expression in the cell-line, consistent with our *in vivo* endometriosis (mouse model) data. This plausibly suggests that TGF-B1 induces EMT via N-cadherin and vimentin expression. However, the purpose of retaining the phosphorylated form of E-cadherin in these cells is still unclear.

Cell migration is a function of EMT, and our *in vivo* and *in vitro* evidence suggests that TGF-B1 could trigger RHOA and RAC1 activity, leading to cell migration in endometriosis [93] via EMT [94]. RHOA and RHOC have already been linked to endometriosis and shown to affect the migratory potential of cells like a cell motility initiating factor [61]. In response to TGF-B1, the elevated level of RHOC might regulate the invasive phenotype of endometrial cells under endometriotic conditions as previously observed [95]. Moreover, RHOC was mainly distributed in the epithelial cells of the PBS/sham-treated animal groups, but its expression intensified in all cell types of the ectopic lesions after TGF-B1 supplementation. Overall, activation of RHOC decreases cell polarity but increases invasion. On the other hand, activation of RHOA inhibits the invasive potential and motility of cells [96] and similar conditions we postulate in the endometriotic cells as well.

A RHOGTPase subtype, RAC1, has been linked to the migration of stromal cells [97], a phenomenon that is certainly taking place in the endometriosis in response to TGF-B1. The

Downloaded from https://academic.oup.com/biolreprod/advance-article-abstract/doi/10.1093/biolre/ioy242/5181331 by EKU Libraries user on 14 November 2018

endometriotic lesions are composed of more stromal cells than epithelial cells. The elevated RAC1 activity suggests that the stromal cells of endometriotic lesions migrate under the influence of the RAC1 signaling axis [98], and cross-talk between the TGF-B1 and RAC1 signaling pathways seems to be leading cause of the progression of endometriosis.

Another subtype of RHOGTPase, RHOG, participates in cell invasion in cancer [99]. The increased mRNA, protein, and activity levels of RHOA, RHOC, RAC1, and RHOG, suggest that they regulate the migratory and invasive phenotypes of endometrial stromal cells. These phenotypes are required to sustain the cells at ectopic sites in the peritoneal endometriosis in response to TGF-B1. This was supported by the TGF-B1-dependent up-regulation of ITGB3, VAV, RAC1, and RHOG observed in human ovarian endometriotic cells (HS.832(C).T) under *in vitro* conditions, as well as in our *in vivo* study.

TGF-B1 supplementation also enhanced the colony formation capacity and invasive potential of human ovarian endometriotic cells. Since transformed uterine stromal (T-HES) cells are less aggressive than the HS.832(C).T cells, we observed that the basal migratory potential of both cell lines was similar, but only HS.832(C).T showed a strong response towards the presence of TGF-B1 in the transwell-matrigel invasion assay. Here, HS.832(C).T endometriotic cells showed higher colonization, migration potential, and invasion capacity than the T-HES cells, suggesting that during the course of endometriosis, these cellular events are accelerated by excessive TGF-B1 exposure.

Furthermore, the colony formation and egression/invasion capacities of both cell types from 3D-spheroids into matrigel were enhanced after TGF-B1 exposure. Herein, the enhanced migration and EMT potential could be due to increased levels of RHOGTPases and N-cadherin respectively. Together, in response to TGF-B1, the elevated expression and/or activity of RAC1,

Downloaded from https://academic.oup.com/biolreprod/advance-article-abstract/doi/10.1093/biolre/ioy242/5181331 by EKU Libraries user on 14 November 2018

RHOC, and RHOG in the peritoneal endometriotic lesions orchestrate the migration of cells to ectopic sites where they adhere with the help of cadherins, colonize, and are sustained. The present information points to TGF-B1-regulation of RHOGTPase subtypes giving rise to an enhanced cell migratory phenotype.

These observations suggest that under the influence of high TGF-B1 levels, endometriotic cells may migrate, attach, proliferate, colonize, and invade the extracellular matrix of mesothelial cells. These sequential cellular events ultimately help in the initiation, progression, and growth of ectopic endometriotic lesions, and TGF-B1 plays a prominent role in endometriosis development. The Hs832 (CRL-7566) cell line was established from a benign ovarian cyst (inner and outer surfaces) of a patient with endometriosis. The cell line is not fully characterized by ATCC, USA; thus, outcome of these cells should be interpreted carefully.

5. Conclusion: *In vivo* and *in vitro* evidence suggests that elevated TGF-B1 is an important regulator of ectopic lesion development in endometriosis. TGF-B1 establishes pelvic endometriosis by specifically enhancing the migration, attachment, proliferation, colonization, and invasion by floating endometriotic cells or tissues, via the Integrin-FAK, cadherin, and RHOGTPase signaling cascades (Fig. S5).

Declaration of interests: The authors declare no conflict of interests.

Author Contributions: U.K.S., contributed in experimental design, in vivo and in vitro experimentation, data analysis, interpretation, manuscript writing. S.B.C. contributed in animal model preparation, immunohistochemistry, interpretation, manuscript writing. and data analysis.

Downloaded from https://academic.oup.com/biolreprod/advance-article-abstract/doi/10.1093/biolre/ioy242/5181331 by EKU Libraries user on 14 November 2018

V.K., and V.U., contributed in figure-3F and 4H and I, respectively. T.K. contributed in figures 6A and G. BSVV provided the figure-4A and B and assisted in the protein sample preparation. R.K., helped in the histological, immunofluorescence, and immunohistochemical analysis and valuable suggestions. H.K.B., and S.S., helped in the histopathological analysis and valuable suggestions. S.K.R assisted in the concept of the study and the financial support. R.K.J., conceptualized, designed the experiments, interpreted the data, wrote manuscript and finalized the manuscript. All authors reviewed the manuscript before submission.

Acknowledgement

The authors would like to thank Dr. J. V. Pratap for the critical comments in the manuscript. We would also like to acknowledge the microtome facility of Dr. Gopal Gupta. Dr. Kavita Singh is acknowledged for technical assistance in Confocal Laser Scanning Microscopy, SAIF. Ms. Kanchan Gupta help in immunostaining score analysis through Image ProPlus 4.0 version is also acknowledged. CSIR-CDRI manuscript communication number is 59/2016/RKJ. The authors acknowledge the Inprint Scientific Editing Services, Washington University, MO, USA.

Reference List

[1] Huhtinen K, Stahle M, Perheentupa A, Poutanen M. Estrogen biosynthesis and signaling in endometriosis. Mol Cell Endocrinol 2012; 358: 146-154.

[2] Giudice LC, Kao LC. Endometriosis. Lancet 2004; 364: 1789-1799.

[3] Sampson JA. Metastatic or Embolic Endometriosis, due to the Menstrual Dissemination of Endometrial Tissue into the Venous Circulation. Am J Pathol 1927; 3: 93-110.

[4] Xiong W, Zhang L, Yu L, Xie W, Man Y, Xiong Y, Liu H, Liu Y. Estradiol promotes cells invasion by activating beta-catenin signaling pathway in endometriosis. Reproduction 2015; 150: 507-516.

[5] Greaves E, Temp J, Esnal-Zufiurre A, Mechsner S, Horne AW, Saunders PT. Estradiol is a critical mediator of macrophage-nerve cross talk in peritoneal endometriosis. Am J Pathol 2015; 185: 2286-2297.

Downloaded from https://academic.oup.com/biolreprod/advance-article-abstract/doi/10.1093/biolre/ioy242/5181331 by EKU Libraries user on 14 November 2018

[6] Hickey M, Ballard K, Farquhar C. Endometriosis. BMJ 2014; %19;348:g1752. doi: 10.1136/bmj.g1752.: g1752.

[7] Beliard A, Noel A, Foidart JM. Reduction of apoptosis and proliferation in endometriosis. Fertil Steril 2004; 82: 80-85.

[8] Young VJ, Ahmad SF, Brown JK, Duncan WC, Horne AW. Peritoneal VEGF-A expression is regulated by TGF-beta1 through an ID1 pathway in women with endometriosis. Sci Rep 2015; 5:16859. doi: 10.1038/srep16859.: 16859.

[9] Young VJ, Brown JK, Saunders PT, Duncan WC, Horne AW. The peritoneum is both a source and target of TGF-beta in women with endometriosis. PLoS One 2014; 9: e106773.

[10] Hull ML, Johan MZ, Hodge WL, Robertson SA, Ingman WV. Host-derived TGFB1 deficiency suppresses lesion development in a mouse model of endometriosis. Am J Pathol 2012; 180: 880-887.

[11] Zhang Q, Duan J, Liu X, Guo SW. Platelets drive smooth muscle metaplasia and fibrogenesis in endometriosis through epithelial-mesenchymal transition and fibroblast-to-myofibroblast transdifferentiation. Mol Cell Endocrinol 2016; 428:1-16. doi: 10.1016/j.mce.2016.03.015. Epub;%2016 Mar 15.: 1-16.

[12] Agic A, Xu H, Finas D, Banz C, Diedrich K, Hornung D. Is endometriosis associated with systemic subclinical inflammation? Gynecol Obstet Invest 2006; 62: 139-147.

[13] Dou Q, Williams RS, Chegini N. Inhibition of transforming growth factor-beta 1 alters the growth, anchor-dependent cell aggregation and integrin mRNA expression in human promonocytes: implications for endometriosis and peritoneal adhesion formation. Mol Hum Reprod 1997; 3: 383-391.

[14] Liu YG, Tekmal RR, Binkley PA, Nair HB, Schenken RS, Kirma NB. Induction of endometrial epithelial cell invasion and c-fms expression by transforming growth factor beta. Mol Hum Reprod 2009; 15: 665-673.

[15] Bacci M, Capobianco A, Monno A, Cottone L, Di PF, Camisa B, Mariani M, Brignole C, Ponzoni M, Ferrari S, Panina-Bordignon P, Manfredi AA, Rovere-Querini P. Macrophages are alternatively activated in patients with endometriosis and required for growth and vascularization of lesions in a mouse model of disease. Am J Pathol 2009; 175: 547-556.

[16] Tamura M, Fukaya T, Enomoto A, Murakami T, Uehara S, Yajima A. Transforming growth factor-beta isoforms and receptors in endometriotic cysts of the human ovary. Am J Reprod Immunol 1999; 42: 160-167.

[17] Loverro G, Maiorano E, Napoli A, Selvaggi L, Marra E, Perlino E. Transforming growth factor-beta 1 and insulin-like growth factor-1 expression in ovarian endometriotic cysts: a preliminary study. Int J Mol Med 2001; 7: 423-429.

[18] Yoshimura A, Wakabayashi Y, Mori T. Cellular and molecular basis for the regulation of inflammation by TGF-beta. J Biochem 2010; 147: 781-792.

Downloaded from https://academic.oup.com/biolreprod/advance-article-abstract/doi/10.1093/biolre/ioy242/5181331 by EKU Libraries user on 14 November 2018

[19] Jakowlew SB. Transforming growth factor-beta in cancer and metastasis. Cancer Metastasis Rev 2006; 25: 435-457.

[20] Heldin CH, Miyazono K, ten DP. TGF-beta signalling from cell membrane to nucleus through SMAD proteins. Nature 1997; 390: 465-471.

[21] Vaidya A, Kale VP. TGF-beta signaling and its role in the regulation of hematopoietic stem cells. Syst Synth Biol 2015; 9: 1-10.

[22] Mori S, Kodaira M, Ito A, Okazaki M, Kawaguchi N, Hamada Y, Takada Y, Matsuura N. Enhanced Expression of Integrin alphavbeta3 Induced by TGF-beta Is Required for the Enhancing Effect of Fibroblast Growth Factor 1 (FGF1) in TGF-beta-Induced Epithelial-Mesenchymal Transition (EMT) in Mammary Epithelial Cells. PLoS One 2015; 10: e0137486.

[23] Beliard A, Donnez J, Nisolle M, Foidart JM. Localization of laminin, fibronectin, E-cadherin, and integrins in endometrium and endometriosis. Fertil Steril 1997; 67: 266-272.

[24] Chan PY, Kanner SB, Whitney G, Aruffo A. A transmembrane-anchored chimeric focal adhesion kinase is constitutively activated and phosphorylated at tyrosine residues identical to pp125FAK. J Biol Chem 1994; 269: 20567-20574.

[25] Mu L, Ma YY. Expression of focal adhesion kinase in endometrial stromal cells of women with endometriosis was adjusted by ovarian steroid hormones. Int J Clin Exp Pathol 2015; 8: 1810-1815.

[26] Chen HC, Appeddu PA, Isoda H, Guan JL. Phosphorylation of tyrosine 397 in focal adhesion kinase is required for binding phosphatidylinositol 3-kinase. J Biol Chem 1996; 271: 26329-26334.

[27] Legate KR, Montanez E, Kudlacek O, Fassler R. ILK, PINCH and parvin: the tIPP of integrin signalling. Nat Rev Mol Cell Biol 2006; 7: 20-31.

[28] Huveneers S, Danen EH. Adhesion signaling - crosstalk between integrins, Src and Rho. J Cell Sci 2009; 122: 1059-1069.

[29] Fleming YM, Ferguson GJ, Spender LC, Larsson J, Karlsson S, Ozanne BW, Grosse R, Inman GJ. TGF-beta-mediated activation of RhoA signalling is required for efficient (V12)HaRas and (V600E)BRAF transformation. Oncogene 2009; %19;28: 983-993.

[30] Li X, Bao Y, Fang P, Chen Y, Qiao Z. Effect of mifepristone on COX-2 both in eutopic and ectopic endometrium in mouse endometriotic model. Arch Gynecol Obstet 2012; 286: 939-946.

[31] Pelch KE, Sharpe-Timms KL, Nagel SC. Mouse model of surgically-induced endometriosis by auto-transplantation of uterine tissue. J Vis Exp 2012; e3396.

[32] Rudzitis-Auth J, Korbel C, Scheuer C, Menger MD, Laschke MW. Xanthohumol inhibits growth and vascularization of developing endometriotic lesions. Hum Reprod 2012; 27: 1735-1744.

Downloaded from https://academic.oup.com/biolreprod/advance-article-abstract/doi/10.1093/biolre/ioy242/5181331 by EKU Libraries user on 14 November 2018

[33] Hirata T, Osuga Y, Yoshino O, Hirota Y, Harada M, Takemura Y, Morimoto C, Koga K, Yano T, Tsutsumi O, Taketani Y. Development of an experimental model of endometriosis using mice that ubiquitously express green fluorescent protein. Hum Reprod 2005; 20: 2092-2096.

[34] Oosterlynck DJ, Meuleman C, Waer M, Koninckx PR. Transforming growth factor-beta activity is increased in peritoneal fluid from women with endometriosis. Obstet Gynecol 1994; 83: 287-292.

[35] Chen QH, Zhou WD, Pu DM, Huang QS, Li T, Chen QX. 15-Epi-lipoxin A(4) inhibits the progression of endometriosis in a murine model. Fertil Steril 2010; 93: 1440-1447.

[36] Chadchan SB, Kumar V, Maurya VK, Soni UK, Jha RK. Endoglin (CD105) coordinates the process of endometrial receptivity for embryo implantation. Mol Cell Endocrinol 2016; 10.

[37] Ubba V, Soni UK, Chadchan S, Maurya VK, Kumar V, Maurya R, Chaturvedi H, Singh R, Dwivedi A, Jha RK. RHOG-DOCK1-RAC1 Signaling Axis Is Perturbed in DHEA-Induced Polycystic Ovary in Rat Model. Reprod Sci 2017; 24: 738-752.

[38] Kumar V, Soni UK, Maurya VK, Singh K, Jha RK. Integrin beta8 (ITGB8) activates VAV-RAC1 signaling via FAK in the acquisition of endometrial epithelial cell receptivity for blastocyst implantation. Sci Rep 2017; 7: 1885-01764.

[39] O'Hayre M, Inoue A, Kufareva I, Wang Z, Mikelis CM, Drummond RA, Avino S, Finkel K, Kalim KW, DiPasquale G, Guo F, Aoki J, Zheng Y, Lionakis MS, Molinolo AA, Gutkind JS. Inactivating mutations in GNA13 and RHOA in Burkitt's lymphoma and diffuse large B-cell lymphoma: a tumor suppressor function for the Galpha13/RhoA axis in B cells. Oncogene 2016; 35: 3771-3780.

[40] Ozkucur N, Quinn KP, Pang JC, Du C, Georgakoudi I, Miller E, Levin M, Kaplan DL. Membrane potential depolarization causes alterations in neuron arrangement and connectivity in cocultures. Brain Behav 2015; 5: 24-38.

[41] Qiu X, Cheng JC, Klausen C, Fan Q, Chang HM, So WK, Leung PC. Transforming growth factor-alpha induces human ovarian cancer cell invasion by down-regulating E-cadherin in a Snail-independent manner. Biochem Biophys Res Commun 2015; 461: 128-135.

[42] Szeto HH, Liu S, Soong Y, Birk AV. Improving mitochondrial bioenergetics under ischemic conditions increases warm ischemia tolerance in the kidney. Am J Physiol Renal Physiol 2015; 308: F11-F21.

[43] Thakur R, Trivedi R, Rastogi N, Singh M, Mishra DP. Inhibition of STAT3, FAK and Src mediated signaling reduces cancer stem cell load, tumorigenic potential and metastasis in breast cancer. Sci Rep 2015; 5:10194. doi: 10.1038/srep10194.: 10194.

[44] Wang X, Chen L, Liu J, Yan T, Wu G, Xia Y, Zong G, Li F. In vivo treatment of rat arterial adventitia with interleukin1beta induces intimal proliferation via the JAK2/STAT3 signaling pathway. Mol Med Rep 2016; 13: 3451-3458.

Downloaded from https://academic.oup.com/biolreprod/advance-article-abstract/doi/10.1093/biolre/ioy242/5181331 by EKU Libraries user on 14 November 2018

[45] Gupta K, Sirohi VK, Kumari S, Shukla V, Manohar M, Popli P, Dwivedi A. Sorcin is involved during embryo implantation via activating VEGF/PI3K/Akt pathway in mice. J Mol Endocrinol 2018; 60: 119-132.

[46] Laemmli UK. Cleavage of structural proteins during the assembly of the head of bacteriophage T4. Nature 1970; 227: 680-685.

[47] Towbin H, Staehelin T, Gordon J. Electrophoretic transfer of proteins from polyacrylamide gels to nitrocellulose sheets: procedure and some applications. 1979. Biotechnology 1992; 24:145-9.: 145-149.

[48] Bzymek R, Horsthemke M, Isfort K, Mohr S, Tjaden K, Muller-Tidow C, Thomann M, Schwerdtle T, Bahler M, Schwab A, Hanley PJ. Real-time two- and three-dimensional imaging of monocyte motility and navigation on planar surfaces and in collagen matrices: roles of Rho. Sci Rep 2016; 6:25016. doi: 10.1038/srep25016.: 25016.

[49] Fan Y, Qu X, Ma Y, Liu Y, Hu X. Cbl-b promotes cell detachment via ubiquitination of focal adhesion kinase. Oncol Lett 2016; 12: 1113-1118.

[50] Gandin V, Masvidal L, Cargnello M, Gyenis L, McLaughlan S, Cai Y, Tenkerian C, Morita M, Balanathan P, Jean-Jean O, Stambolic V, Trost M, Furic L, Larose L, Koromilas AE, Asano K, Litchfield D, Larsson O, Topisirovic I. mTORC1 and CK2 coordinate ternary and eIF4F complex assembly. Nat Commun 2016; 7:11127. doi: 10.1038/ncomms11127.: 11127.

[51] Kumar V, Maurya VK, Joshi A, Meeran SM, Jha RK. Integrin beta 8 (ITGB8) regulates embryo implantation potentially via controlling the activity of TGF-B1 in mice. Biol Reprod 2015; 92: 109.

[52] Liu J, Wan L, Liu J, Yuan Z, Zhang J, Guo J, Malumbres M, Liu J, Zou W, Wei W. Cdh1 inhibits WWP2-mediated ubiquitination of PTEN to suppress tumorigenesis in an APC-independent manner. Cell Discov 2016; 2:15044. doi: 10.1038/celldisc.2015.44. eCollection;%2016.: 15044.

[53] Maurya VK, Jha RK, Kumar V, Joshi A, Chadchan S, Mohan JJ, Laloraya M. Transforming growth factor-beta 1 (TGF-B1) liberation from its latent complex during embryo implantation and its regulation by estradiol in mouse. Biol Reprod 2013; 89: 84.

[54] Maurya VK, Sangappa C, Kumar V, Mahfooz S, Singh A, Rajender S, Jha RK. Expression and activity of Rac1 is negatively affected in the dehydroepiandrosterone induced polycystic ovary of mouse. J Ovarian Res 2014; 7:32. doi: 10.1186/1757-2215-7-32.: 32-37.

[55] McGuire VA, Ruiz-Zorrilla DT, Emmerich CH, Strickson S, Ritorto MS, Sutavani RV, Weibeta A, Houslay KF, Knebel A, Meakin PJ, Phair IR, Ashford ML, Trost M, Arthur JS. Dimethyl fumarate blocks pro-inflammatory cytokine production via inhibition of TLR induced M1 and K63 ubiquitin chain formation. Sci Rep 2016; 6:31159. doi: 10.1038/srep31159.: 31159.

[56] Nakamura A, Yoshida K, Ueda H, Takeda S, Ikeda S. Up-regulation of mitogen activated protein kinases in mdx skeletal muscle following chronic treadmill exercise. Biochim Biophys Acta 2005; 1740: 326-331.

Downloaded from https://academic.oup.com/biolreprod/advance-article-abstract/doi/10.1093/biolre/ioy242/5181331 by EKU Libraries user on 14 November 2018

[57] Wang Y, Chen Y, Wu M, Lan T, Wu Y, Li Y, Qian H. Type II cyclic guanosine monophosphate-dependent protein kinase inhibits Rac1 activation in gastric cancer cells. Oncol Lett 2015; 10: 502-508.

[58] Rao X, Huang X, Zhou Z, Lin X. An improvement of the 2^(-delta delta CT) method for quantitative real-time polymerase chain reaction data analysis. Biostat Bioinforma Biomath 2013; 3(3): 71-85.

[59] Colon-Diaz M, Baez-Vega P, Garcia M, Ruiz A, Monteiro JB, Fourquet J, Bayona M, Alvarez-Garriga C, Achille A, Seto E, Flores I. HDAC1 and HDAC2 are differentially expressed in endometriosis. Reprod Sci 2012; 19: 483-492.

[60] Ono YJ, Terai Y, Tanabe A, Hayashi A, Hayashi M, Yamashita Y, Kyo S, Ohmichi M. Decorin induced by progesterone plays a crucial role in suppressing endometriosis. J Endocrinol 2014; 223: 203-216.

[61] Jiang QY, Xia JM, Ding HG, Fei XW, Lin J, Wu RJ. RNAi-mediated blocking of ezrin reduces migration of ectopic endometrial cells in endometriosis. Mol Hum Reprod 2012; 18: 435-441.

[62] Cabinakova M, Mikulova V, Malickova K, Vrana D, Pavlista D, Petruzelka L, Zima T, Tesarova P. Predictive factors for the presence of tumor cells in bone marrow and peripheral blood in breast cancer patients. Neoplasma 2015; 62: 259-268.

[63] Fournier AK, Campbell LE, Castagnino P, Liu WF, Chung BM, Weaver VM, Chen CS, Assoian RK. Rac-dependent cyclin D1 gene expression regulated by cadherin- and integrin-mediated adhesion. J Cell Sci 2008; 121: 226-233.

[64] Dios-Esponera A, Isern d, V, Sevilla-Movilla S, Garcia-Verdugo R, Garcia-Bernal D, Arellano-Sanchez N, Cabanas C, Teixido J. Positive and negative regulation by SLP-76/ADAP and Pyk2 of chemokine-stimulated T-lymphocyte adhesion mediated by integrin alpha4beta1. Mol Biol Cell 2015; 26: 3215-3228.

[65] McCloy RA, Rogers S, Caldon CE, Lorca T, Castro A, Burgess A. Partial inhibition of Cdk1 in G 2 phase overrides the SAC and decouples mitotic events. Cell Cycle 2014; 13(9): 1400-1412.

[66] Lo BN, Parrotta R, Morone S, Bovino P, Nacci G, Ortolan E, Horenstein AL, Inzhutova A, Ferrero E, Funaro A. The CD157-integrin partnership controls transendothelial migration and adhesion of human monocytes. J Biol Chem 2011; 286: 18681-18691.

[67] Jaskolski F, Mulle C, Manzoni OJ. An automated method to quantify and visualize colocalized fluorescent signals. J Neurosci Methods 2005; 146: 42-49.

[68] Gao J, Zhu Y, Nilsson M, Sundfeldt K. TGF-beta isoforms induce EMT independent migration of ovarian cancer cells. Cancer Cell Int 2014; 14(1): 72-0072.

[69] Berens EB, Holy JM, Riegel AT, Wellstein A. A Cancer Cell Spheroid Assay to Assess Invasion in a 3D Setting. J Vis Exp 2015; %20;(105). doi: 10.

Downloaded from https://academic.oup.com/biolreprod/advance-article-abstract/doi/10.1093/biolre/ioy242/5181331 by EKU Libraries user on 14 November 2018

[70] Zhou WD, Yang HM, Wang Q, Su DY, Liu FA, Zhao M, Chen QH, Chen QX. SB203580, a p38 mitogen-activated protein kinase inhibitor, suppresses the development of endometriosis by down-regulating proinflammatory cytokines and proteolytic factors in a mouse model. Hum Reprod 2010; 25: 3110-3116.

[71] Zhang H, Zhao X, Liu S, Li J, Wen Z, Li M. 17betaE2 promotes cell proliferation in endometriosis by decreasing PTEN via NFkappaB-dependent pathway. Mol Cell Endocrinol 2010; 317: 31-43.

[72] Sundqvist J, Andersson KL, Scarselli G, Gemzell-Danielsson K, Lalitkumar PG. Expression of adhesion, attachment and invasion markers in eutopic and ectopic endometrium: a link to the aetiology of endometriosis. Hum Reprod 2012; 27(9): 2737-2746.

[73] Zhang Q, Dong P, Liu X, Sakuragi N, Guo SW. Enhancer of Zeste homolog 2 (EZH2) induces epithelial-mesenchymal transition in endometriosis. Sci Rep 2017; 7: 6804-06920.

[74] Matsuzaki S, Darcha C, Pouly JL, Canis M. Effects of matrix stiffness on epithelial to mesenchymal transition-like processes of endometrial epithelial cells: Implications for the pathogenesis of endometriosis. Sci Rep 2017; 7:44616. doi: 10.1038/srep44616.: 44616.

[75] Yotova IY, Quan P, Leditznig N, Beer U, Wenzl R, Tschugguel W. Abnormal activation of Ras/Raf/MAPK and RhoA/ROCKII signalling pathways in eutopic endometrial stromal cells of patients with endometriosis. Hum Reprod 2011; 26: 885-897.

[76] Meola J, Dentillo DB, Rosa e Silva JC, Hidalgo GS, Paz CC, Ferriani RA. RHOC: a key gene for endometriosis. Reprod Sci 2013; 20: 998-1002.

[77] Liu H, Zhang Z, Xiong W, Zhang L, Xiong Y, Li N, He H, Du Y, Liu Y. Hypoxia-inducible factor-1alpha promotes endometrial stromal cells migration and invasion by upregulating autophagy in endometriosis. Reproduction 2017; 153: 809-820.

[78] Tipps AM, Plaxe SC, Weidner N. Endometrioid carcinoma with a low-grade spindle cell component: a tumor resembling an adnexal tumor of probable Wolffian origin. Ann Diagn Pathol 2011; 15: 376-381.

[79] Bulun SE. Endometriosis. N Engl J Med 2009; 360: 268-279.

[80] Kyama CM, Overbergh L, Mihalyi A, Meuleman C, Mwenda JM, Mathieu C, D'Hooghe TM. Endometrial and peritoneal expression of aromatase, cytokines, and adhesion factors in women with endometriosis. Fertil Steril 2008; 89: 301-310.

[81] Au HK, Chang JH, Wu YC, Kuo YC, Chen YH, Lee WC, Chang TS, Lan PC, Kuo HC, Lee KL, Lee MT, Tzeng CR, Huang YH. TGF-betaI Regulates Cell Migration through Pluripotent Transcription Factor OCT4 in Endometriosis. PLoS One 2015; 10: e0145256.

[82] Komiyama S, Aoki D, Komiyama M, Nozawa S. Local activation of TGF-beta1 at endometriosis sites. J Reprod Med 2007; 52: 306-312.

[83] Dela CC, Reis FM. The role of TGFbeta superfamily members in the pathophysiology of endometriosis. Gynecol Endocrinol 2015; 31: 511-515.

Downloaded from https://academic.oup.com/biolreprod/advance-article-abstract/doi/10.1093/biolre/ioy242/5181331 by EKU Libraries user on 14 November 2018

[84] Grummer R. Animal models in endometriosis research. Hum Reprod Update 2006; 12: 641-649.

[85] Bakin AV, Rinehart C, Tomlinson AK, Arteaga CL. p38 mitogen-activated protein kinase is required for TGFbeta-mediated fibroblastic transdifferentiation and cell migration. J Cell Sci 2002; 115: 3193-3206.

[86] Govatati S, Kodati VL, Deenadayal M, Chakravarty B, Shivaji S, Bhanoori M. Mutations in the PTEN tumor gene and risk of endometriosis: a case-control study. Hum Reprod 2014; 29: 324-336.

[87] Fragoso R, Barata JT. Kinases, tails and more: regulation of PTEN function by phosphorylation. Methods 2015; 77-78:75-81. doi: 10.1016/j.ymeth.2014.10.015. Epub;%2014 Oct 22.: 75-81.

[88] Vazquez F, Ramaswamy S, Nakamura N, Sellers WR. Phosphorylation of the PTEN tail regulates protein stability and function. Mol Cell Biol 2000; 20: 5010-5018.

[89] Klemmt PA, Carver JG, Koninckx P, McVeigh EJ, Mardon HJ. Endometrial cells from women with endometriosis have increased adhesion and proliferative capacity in response to extracellular matrix components: towards a mechanistic model for endometriosis progression. Hum Reprod 2007; 22: 3139-3147.

[90] Mu L, Zheng W, Wang L, Chen XJ, Zhang X, Yang JH. Alteration of focal adhesion kinase expression in eutopic endometrium of women with endometriosis. Fertil Steril 2008; 89: 529-537.

[91] Tange S, Oktyabri D, Terashima M, Ishimura A, Suzuki T. JARID2 is involved in transforming growth factor-beta-induced epithelial-mesenchymal transition of lung and colon cancer cell lines. PLoS One 2014; 9: e115684.

[92] Chen CL, Wang SH, Chan PC, Shen MR, Chen HC. Phosphorylation of E-cadherin at threonine 790 by protein kinase Cdelta reduces beta-catenin binding and suppresses the function of E-cadherin. Oncotarget 2016; 10.

[93] Kim HJ, Kim JG, Moon MY, Park SH, Park JB. IkappaB kinase gamma/nuclear factor-kappaB-essential modulator (IKKgamma/NEMO) facilitates RhoA GTPase activation, which, in turn, activates Rho-associated KINASE (ROCK) to phosphorylate IKKbeta in response to transforming growth factor (TGF)-beta1. J Biol Chem 2014; 289: 1429-1440.

[94] Tavares AL, Mercado-Pimentel ME, Runyan RB, Kitten GT. TGF beta-mediated RhoA expression is necessary for epithelial-mesenchymal transition in the embryonic chick heart. Dev Dyn 2006; 235: 1589-1598.

[95] Mukai M, Endo H, Iwasaki T, Tatsuta M, Togawa A, Nakamura H, Inoue M. RhoC is essential for TGF-beta1-induced invasive capacity of rat ascites hepatoma cells. Biochem Biophys Res Commun 2006; 346: 74-82.

[96] Simpson KJ, Dugan AS, Mercurio AM. Functional analysis of the contribution of RhoA and RhoC GTPases to invasive breast carcinoma. Cancer Res 2004; 64: 8694-8701.

Downloaded from https://academic.oup.com/biolreprod/advance-article-abstract/doi/10.1093/biolre/ioy242/5181331 by EKU Libraries user on 14 November 2018

[97] Grewal S, Carver JG, Ridley AJ, Mardon HJ. Implantation of the human embryo requires Rac1-dependent endometrial stromal cell migration. Proc Natl Acad Sci U S A 2008; 105: 16189-16194.

[98] Bousquet E, Calvayrac O, Mazieres J, Lajoie-Mazenc I, Boubekeur N, Favre G, Pradines A. RhoB loss induces Rac1-dependent mesenchymal cell invasion in lung cells through PP2A inhibition. Oncogene 2015; 10.

[99] Kwiatkowska A, Didier S, Fortin S, Chuang Y, White T, Berens ME, Rushing E, Eschbacher J, Tran NL, Chan A, Symons M. The small GTPase RhoG mediates glioblastoma cell invasion. Mol Cancer 2012; 11:65. doi: 10.1186/1476-4598-11-65.: 65-11.

Downloaded from https://academic.oup.com/biolreprod/advance-article-abstract/doi/10.1093/biolre/ioy242/5181331 by EKU Libraries user on 14 November 2018

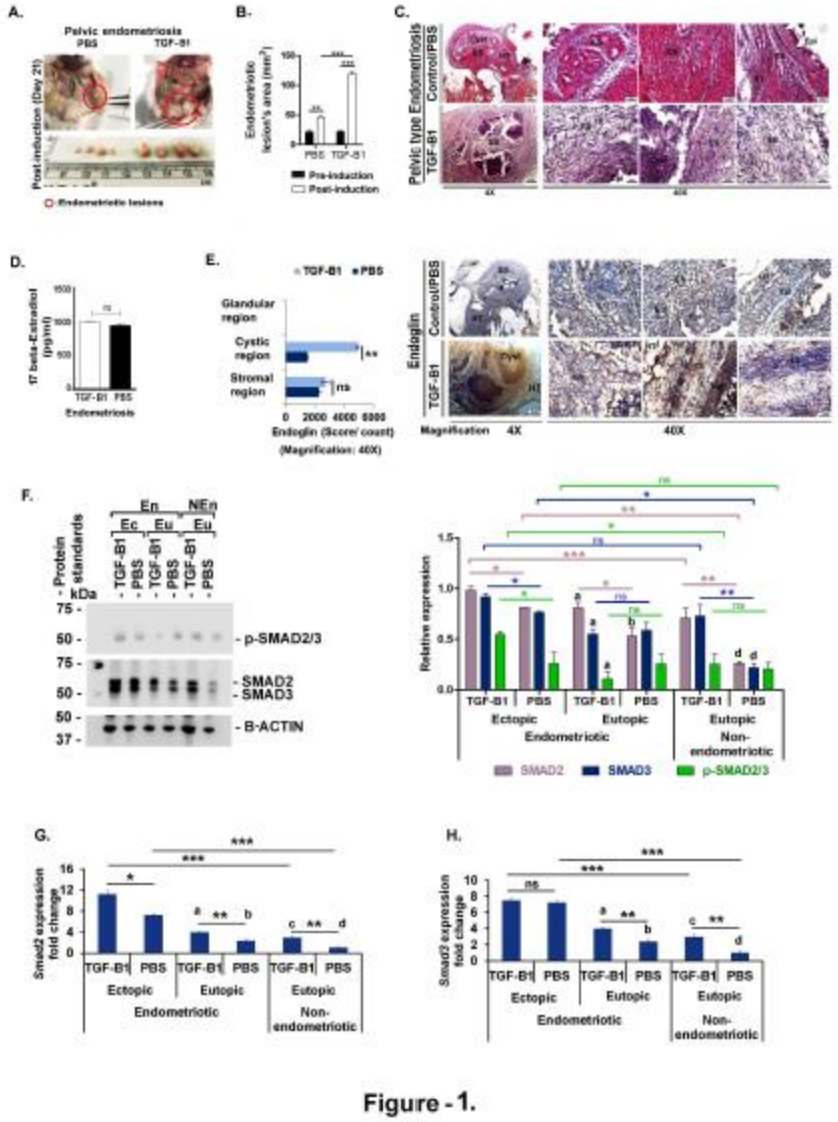

Figure - 1.

Figure- 1: TGF-B1 leads to aggravation of endometriotic lesions in the peritoneal regions and switches on downstream signaling pathways in surgically-implanted autologous endometrial tissue in a mouse model of endometriosis. (A) Animals underwent surgical autologous transplantation of endometrial tissues at the pelvic wall. One week later, animals were treated for two weeks with active recombinant mTGF-B1 or PBS as control/sham. Macroscopically, endometriotic lesions were observed in the peritoneal regions of PBS/sham control and TGF-B1-treated endometriosis mouse models. (B) The average lesional area of all

Downloaded from https://academic.oup.com/biolreprod/advance-article-abstract/doi/10.1093/biolre/ioy242/5181331 by EKU Libraries user on 14 November 2018

replicates was plotted in the form of a bar graph. (C) Hematoxylin and eosin staining was used to histologically characterize the lesions of peritoneal endometriosis in response to TGF-B1. (D) 17-beta-estradiol level in endometriotic lesions from the peritoneal area was measured by ELISA. (E) Increased immunostaining of endoglin (CD105) was seen in the cystic region and stromal cells of tissue sections from the endometriotic lesions of TGF-B1-treated animals compared to the control group. The difference in scores was significant only for the cystic region. Images of the immunohistochemistry were captured at 4X and 40X magnification using an inverted phase-contrast microscope. (F) Immunoblotting and densitometric analyses showed the levels of total SMAD2/3 and p-SMAD2/3 in the eutopic (endometriosis and non-endometriosis) and ectopic endometrial tissues (endometriosis), in response to TGF-B1 supplementation. (G and H) Q-PCR was also performed to measure *Smad2* and *Smad3* transcript levels. Scale bars: 80 μm (4X) and 8 μm (40X). Cyst: Endometrial cyst; EG: Endometrial glands; BV: Blood vessels; Epi: Epithelial tissue; ES: Endometrial stroma; HT: Host tissue. Statistical significance was determined as described in section 2.5. * *($p < 0.05$)*, ** *($p < 0.001$)*, *** *($p < 0.0001$)*. At least three replicates (individual animal as a replicate) were used in each group. The following comparisons were performed: a) TGF-B1-treated ectopic versus eutopic endometrial tissues (endometriosis groups), b) PBS-treated ectopic versus eutopic endometrial tissues (endometriosis groups), c) TGF-B1-treated eutopic endometrial tissue from endometriosis versus non-endometriosis groups, and d) PBS-treated eutopic endometrial tissue from endometriosis versus non-endometriosis groups *($p < 0.01$* for all comparisons*)*. En – endometriosis; NEn – non-endometriosis; Ec – ectopic endometrial tissue; Eu – eutopic endometrial tissue.

Downloaded from https://academic.oup.com/biolreprod/advance-article-abstract/doi/10.1093/biolre/ioy242/5181331 by EKU Libraries user on 14 November 2018

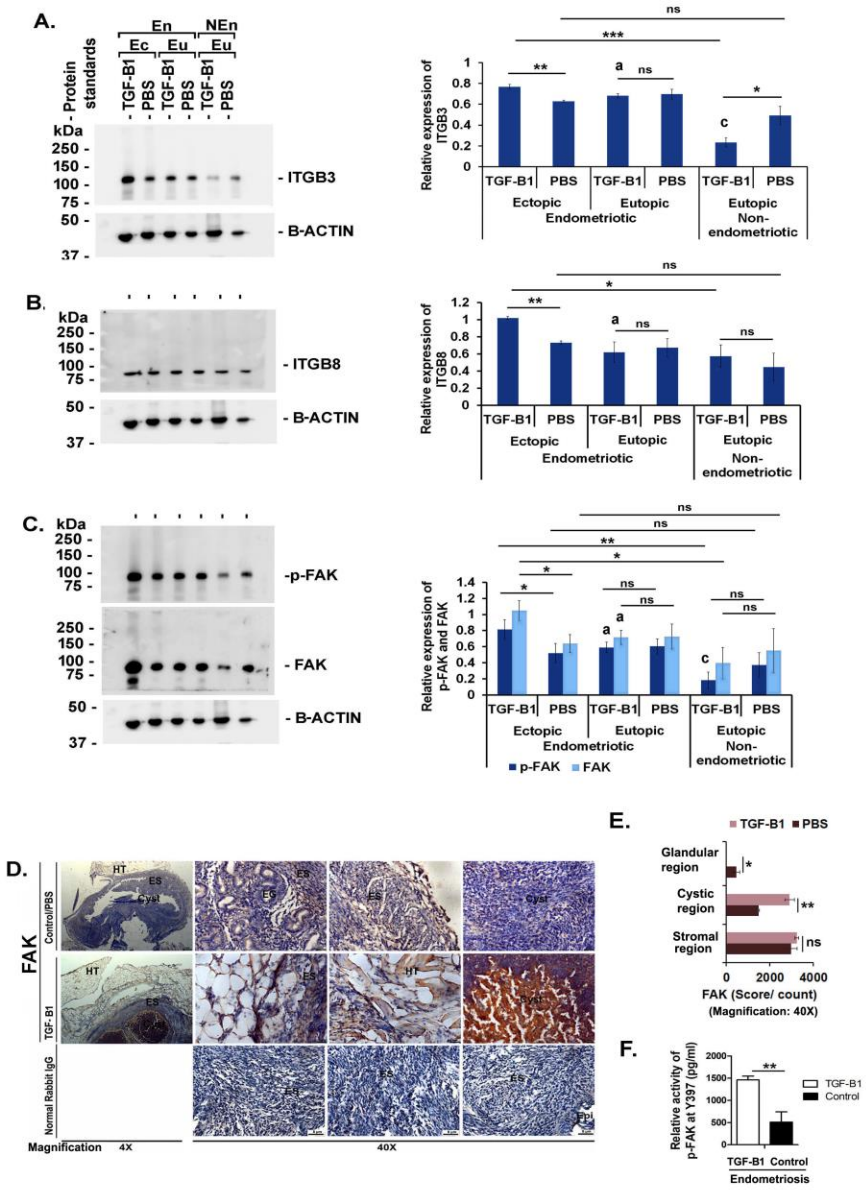

Figure - 2.

Figure- 2: TGF-B1 supplementation promotes the development of peritoneal endometriosis via the integrin-FAK signaling pathway. Immunoblotting and densitometric analyses were performed to assess (A) ITGB3, (B) ITGB8, and (C) p-FAK and FAK expression in the ectopic and eutopic endometrial tissues (TGF-B1- or PBS-treated) from animals with endometriosis, as well as eutopic endometrial tissue from animals without endometriosis. Immunoblots represent

Downloaded from https://academic.oup.com/biolreprod/advance-article-abstract/doi/10.1093/biolre/ioy242/5181331 by EKU Libraries user on 14 November 2018

three independent experiments (individual animal as a replicate). Graphs indicate relative band intensities of specific molecules after normalization to B-actin. (D and E) Immunolocalization of FAK was performed in tissue sections of ectopic lesions from animals with endometriosis, post-PBS- or TGF-B1-treatment to examine the cellular distribution. The immunostaining was quantified by Image Pro Plus 4.0 software and the score/count was plotted in a bar graph Normal rabbit IgG, used a negative control, did not show any significant staining in the tissue. (F) To assess FAK activity, an ELISA for FAK phosphorylation at Tyrosine 397 (Y-397) was performed in endometriotic lesions of animals with endometriosis after TGF-B1 or PBS supplementation. Immunolocalization related images were captured at 4X and 40X magnification, Scale bars: 80 μm (4X) and 8 μm (40X). Cyst: Endometrial cyst; EG: Endometrial glands; BV: Blood vessels; Epi: Epithelial tissue; ES: Endometrial stroma; HT: Host tissue. Statistical significance was determined as described in the section 2.5. * *(p <0.05)*, ** *(p <0.001)*, *** *(p <0.0001*). At least three replicates (individual animal as a replicate) were used in each group. The following comparisons were performed: a) TGF-B1-treated ectopic versus eutopic endometrial tissues (endometriosis groups) and c) TGF-B1-treated eutopic endometrial tissue of animals with endometriosis versus without endometriosis *(p<0.01)*. En – endometriosis; NEn – non-endometriosis; Ec – ectopic endometrial tissue; Eu – eutopic endometrial tissue.

Downloaded from https://academic.oup.com/biolreprod/advance-article-abstract/doi/10.1093/biolre/ioy242/5181331 by EKU Libraries user on 14 November 2018

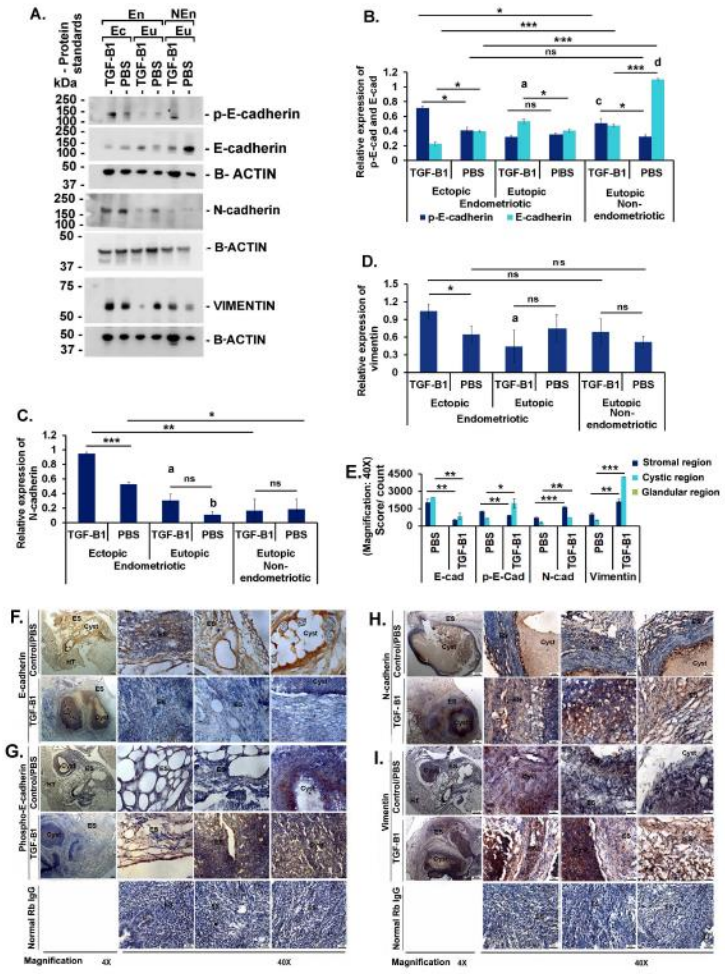

Figure - 3.

Figure- 3: Externally supplemented TGF-B1 promotes expression of EMT biomarkers, N-cadherin and vimentin, in endometriotic lesions from peritoneal endometriosis. Immunoblotting and densitometry analyses were performed to assess the expression of (A and B) E-cadherin, phospho-E-cadherin, (A and C) N-cadherin, and (A and D) vimentin in ectopic and eutopic endometrial tissues (TGF-B1- or PBS-treated) of animals with endometriosis, as well as eutopic endometrial tissues of animals without endometriosis. Densitometric means (with SEM), representing the relative band intensities normalized to B-actin, were plotted in bar graphs.

Downloaded from https://academic.oup.com/biolreprod/advance-article-abstract/doi/10.1093/biolre/ioy242/5181331 by EKU Libraries user on 14 November 2018

Images are representative of three independent experiments (individual animals as replicates). Cell-specific immunolocalization of (F) E-cadherin, (G) phospho-E-cadherin, (H) N-cadherin and (I) vimentin was performed in tissue sections of endometriotic lesions from animals with endometriosis after PBS or TGF-B1 treatment, then quantified using Image Pro Plus 4.0 software and expressed in terms of (E) Score/count. Normal rabbit IgG (negative control) did not show any significant staining in the endometrial tissue. Scale bars: 80 μm (4X) and 8 μm (40X). Cyst: Endometrial cyst; EG: Endometrial glands; BV: Blood vessels; Epi: Epithelial tissue; ES: Endometrial stroma; HT: Host tissue. Statistical significance was determined as described in the section 2.5.* *($p < 0.05$), ** ($p < 0.001$), *** ($p < 0.0001$*). At least three replicates (individual animal as a replicate) were used in each group. The following comparisons were performed: a) TGF-B1-treated ectopic versus eutopic endometrial tissues (endometriosis groups), b) PBS-treated ectopic versus eutopic endometrial tissues (endometriosis groups), c) TGF-B1-treated eutopic endometrial tissue from endometriosis versus non-endometriosis groups, and d) PBS-treated eutopic endometrial tissue from endometriosis versus non-endometriosis groups *($p<0.01$).* NEn – non-endometriosis; Ec – ectopic endometrial tissue; Eu – eutopic endometrial tissue.

Downloaded from https://academic.oup.com/biolreprod/advance-article-abstract/doi/10.1093/biolre/ioy242/5181331 by EKU Libraries user on 14 November 2018

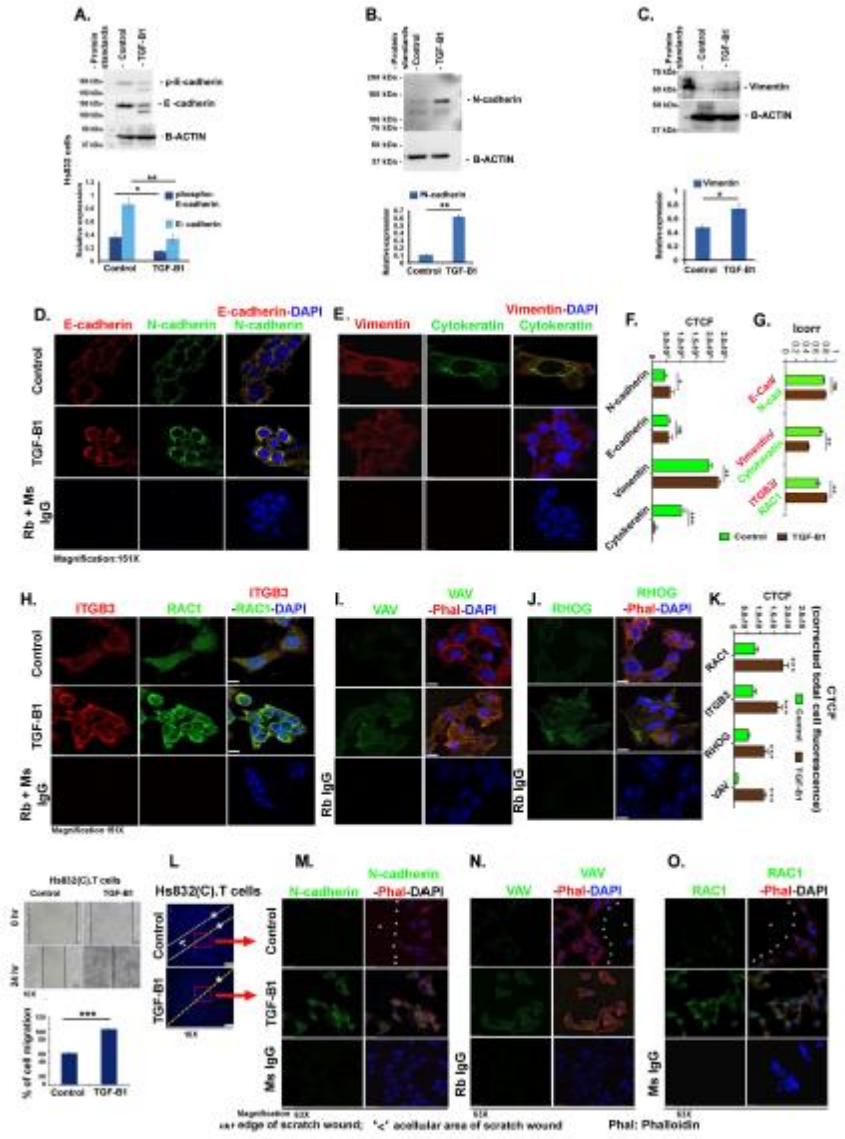

Figure - 4.

Figure- 4: TGF-B1, along with ITGB3, RAC1, VAV, and RHOG, drives epithelial-mesenchymal transition by promoting the mesenchymal markers (N-cadherin and vimentin) and suppressing the epithelial markers (E-cadherin and cytokeratin) in the human ovary/benign cyst endometriotic cells (HS.832(C).T). Expression levels of (A) phosphorylated E-cadherin, E-cadherin, (reprobed with E-cadherin antibody after stripping of phospho-E-cadherin blot), (B) N-cadherin, and (C) vimentin in the HS.832(C).T cells were

Downloaded from https://academic.oup.com/biolreprod/advance-article-abstract/doi/10.1093/biolre/ioy242/5181331 by EKU Libraries user on 14 November 2018

assessed by immunoblotting post-TGF-B1 treatment (24 hours). Blots are representative of three independent experiments. Additionally, we co-localized (D) E-cadherin (red) and N-cadherin (green), in HS.832(C).T cells after 24 hours of treatment with TGF-B1; images were captured by confocal laser scanning microscopy at 63X and 151X magnification in oil. (E) We co-localized vimentin (red), and cytokeratin (green), and counter stained with DAPI (blue) in HS.832(C).T cells after 24 hours of treatment with TGF-B1. (F) N-cadherin, E-cadherin, vimentin, and cytokeratin corrected total cell fluorescence (CTCF) values were calculated from the integrated density of confocal laser scanning microscope images (at least three independent fields of each replicate) by ImageJ1.46r software (NIH) as described in section 2.3.2. Normal rabbit IgG (Rb) for ITGB3, E-cad, vimentin and RHOG, whereas normal mouse IgG (Ms) conjugated with AF488 for N-cad and Cytokeratin were used as isotype controls. DAPI (blue) was used as a nuclear stain. (H-J) Similarly, localization of ITGB3, RAC1, VAV, and RHOG in the HS.832(C).T cells was studied after 24 hour treatment with rh-TGF-B1. (G) The merged fluorescence data of co-localization analyzed for index of correlation (Icorr) from figures for E-cadherin/ N-cadherin (*D*), vimentin/cytokeratin (*E*) and ITGB3 / RAC1 (*H*). The Icorr was quantified by ImgaeJ software. (H) Colocalization of ITGB3 (red) and RAC1 (green), (I) VAV (green) and phalloidin-stained cytoskeleton (red), and (J) RHOG (green) and phalloidin-stained cytoskeleton (red) were analyzed by confocal laser scanning microscopy. (K) Fluorescence intensity was quantified and presented in terms of CTCF. (L) HS.832(C).T cell migration was assayed using the scratched wound healing assay in the presence or absence of TGF-B1 for 24 hr. The wound closure was analyzed after 24 hr and % migration was plotted. The arrow head indicates the acellular area (gap), and asterisks represent the edge of the scratched wound. In the wound healing assay, the focus was mainly on cells present at the edge of the wound that formed

Downloaded from https://academic.oup.com/biolreprod/advance-article-abstract/doi/10.1093/biolre/ioy242/5181331 by EKU Libraries user on 14 November 2018

the migration waves, since these would primarily be the cells that migrate in order to fill the gap created by scratching the cell monolayer. (L and M) Images of cells present at the edge of the scratched wound (indicated by red square) and localized N-cadherin expression (green) along with phalloidin-stained cytoskeleton (red) were captured at 63X and 151X magnification (scale bars: 25μm). For the HS.832(C).T *in vitro* scratch wound healing assay, we focused on cells at the edge of the scratched wound (indicated by asterisk) and captured images by confocal microscopy (indicated by red square) at 63X objective magnification in oil to localize (N**)** VAV and (O) RAC1. DAPI and rhodamine-labelled phalloidin (red) were used as a nuclear stain and a cytoskeleton stain respectively. Isotype controls (For VAV; Normal rabbit IgG along with AF488 conjugated anti-rabbit secondary antibody; for RAC1- normal mouse IgG-AF488) were used as negative controls (lower panels of N and O). Images are representative of three independent experiments. Statistical significance was determined as described in the section 2.5.* *(p <0.05), ** (p <0.001), *** (p <0.0001).* Student's *t-test* was performed for comparisons between control- and TGF-B1-treated groups.

Downloaded from https://academic.oup.com/biolreprod/advance-article-abstract/doi/10.1093/biolre/ioy242/5181331 by EKU Libraries user on 14 November 2018

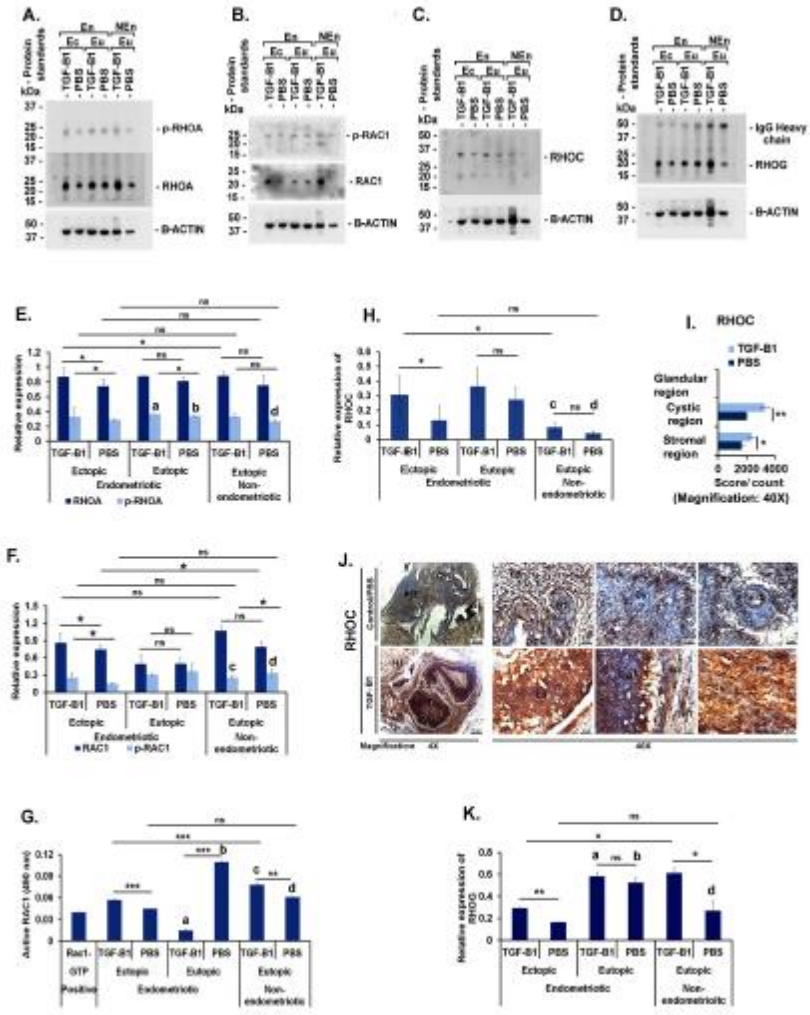

Figure - 5.

Figure- 5: TGF-B1 activates RHOGTPases in the ectopically growing endometrial tissue of peritoneal endometriosis in mice. Immunoblotting and densitometric analysis revealed differential expression of (A and E) p-RHOA and RHOA, (B and F) RAC1 and p-RAC1, (C and H) RHOC, and (D and K) RHOG in the ectopic and eutopic endometrial tissues of animals with endometriosis compared to the eutopic endometrial tissue of animals without endometriosis, after

Downloaded from https://academic.oup.com/biolreprod/advance-article-abstract/doi/10.1093/biolre/ioy242/5181331 by EKU Libraries user on 14 November 2018

TGF-B1 treatment. (G) We assayed the GTP-bound form of RAC1 in the above tissues after TGF-B1 or PBS supplementation. (I and J) Localization of RHOC was performed in tissue sections of endometriotic lesions from the TGF-B1- or PBS-treated animal models of peritoneal endometriosis. The tissue labeled with normal rabbit IgG did not show any significant staining. Scale bars: 80 μm (4X) and 8 μm (40X). Immunostaining of images was quantified and presented as mean score/count and SEM as described in section 2.1.4. Cyst: Endometrial cyst; EG: Endometrial glands; BV: Blood Vessels; Epi: Epithelial tissue; ES: Endometrial Stroma; HT: Host tissue. Statistical significance was determined as described in the section 2.5. * *($p < 0.05$), ** ($p < 0.001$), *** ($p < 0.0001$*). At least three replicates (individual animal as a replicate) were used in each group. The following comparisons were performed: a) TGF-B1-treated ectopic versus eutopic endometrial tissues (endometriosis groups), b) PBS-treated ectopic versus eutopic endometrial tissues (endometriosis groups), c) TGF-B1-treated eutopic endometrial tissue from endometriosis versus non-endometriosis groups, and d) PBS-treated eutopic endometrial tissue from endometriosis versus non-endometriosis groups *($p<0.01$).* En – endometriosis; NEn – non-endometriosis; Ec – ectopic endometrial tissue; Eu – eutopic endometrial tissue.

Downloaded from https://academic.oup.com/biolreprod/advance-article-abstract/doi/10.1093/biolre/ioy242/5181331 by EKU Libraries user on 14 November 2018

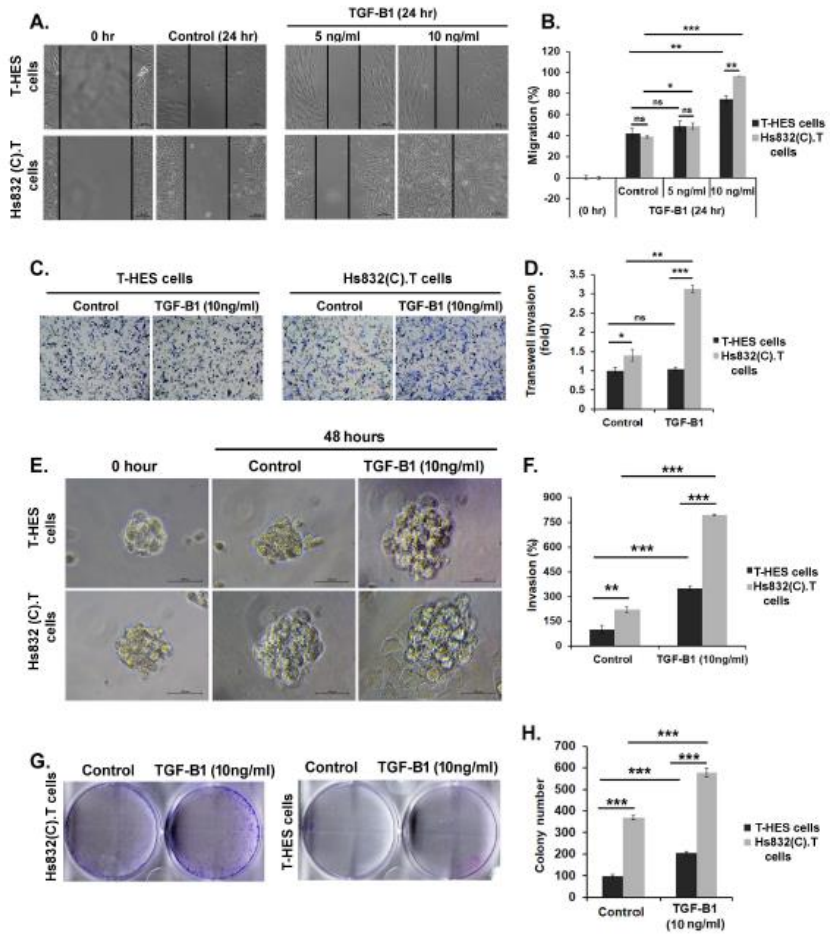

Figure - 6.

Figure-6: TGF-B1 enhances the migration, invasion, and colonization potentials of both human ovarian endometriotic (HS.832(C).T) and non-endometriotic stromal cells (T-HEST). Here, we used T-HES cell line as a non-endometriotic cell control as previously described. (A) Scratch wound closure in response to TGF-B1 was examined in the HS.832(C).T and T-HEST cells. (B) Data were expressed as percent wound closure in treatment groups compared to control. (C) Invasion by endometriotic cells (HS.832(C).T) and T-HEST cells was

Downloaded from https://academic.oup.com/biolreprod/advance-article-abstract/doi/10.1093/biolre/ioy242/5181331 by EKU Libraries user on 14 November 2018

assayed using matrigel-coated Boyden's chambers in response to TGF-B1 treatment for 48 hr. Images of invading cells were captured and total numbers of invading cells were counted in 10 different microscopic fields. (D) Data from treatment and control groups were expressed as number of invasive cells per field. (E) The egression/invasion of cells from the 3D-spheroids into the matrigel in response to TGF-B1 (10 ng/ml) was monitored by measuring the distance of the cells from the edge of the spheroids. (F) Data were plotted as percent invasion compared to control. (G) Colony formation capacities of HS.832(C).T and T-HEST cells were checked after treatment **(**48 hr**)** with TGF-B1 (5 and 10 ng/ml) followed by incubation for 10 days. (H) Data were presented as the mean number of colonies (colonies per well were counted in three independent experiments) and S.E.M. The basal capacities for proliferation, migration, and invasion were higher in the HS.832(C).T cells compared to the T-HEST cells**.** Statistical significance was determined as described in section 2.5.* *(p <0.05), ** (p <0.001), *** (p <0.0001*). Data were collected from at least three independent experiments**.** Scale bars represent 100 μm at 10X magnification for the migration and transwell invasion assays and 20X magnification for 3d-spheroid invasion assay.

Downloaded from https://academic.oup.com/biolreprod/advance-article-abstract/doi/10.1093/biolre/ioy242/5181331 by EKU Libraries user on 14 November 2018